Accepted Manuscript

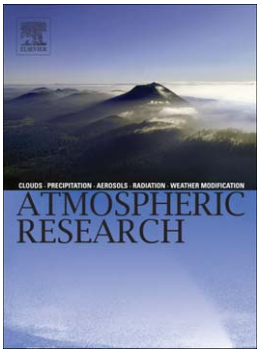

Drought forecasting in eastern Australia using multivariate adaptive regression spline, least square support vector machine and M5Tree model

Ravinesh C Deo, Ozgur Kisi, Vijay P Singh

PII: S0169-8095(16)30450-1
DOI: doi:10.1016/j.atmosres.2016.10.004
Reference: ATMOS 3805

To appear in: *Atmospheric Research*

Received date: 5 July 2016
Revised date: 4 October 2016
Accepted date: 10 October 2016

Please cite this article as: Deo, Ravinesh C, Kisi, Ozgur, Singh, Vijay P, Drought forecasting in eastern Australia using multivariate adaptive regression spline, least square support vector machine and M5Tree model, *Atmospheric Research* (2016), doi:10.1016/j.atmosres.2016.10.004

Drought forecasting in eastern Australia using multivariate adaptive regression spline, least square support vector machine and M5Tree model

Ravinesh C Deo[1 *], Ozgur Kisi[2], Vijay P Singh[3]

[1] School of Agricultural Computational and Environmental Sciences

International Centre of Applied Climate Sciences (ICACS)

University of Southern Queensland, Springfield, AUSTRALIA

*Corresponding Author: ravinesh.deo@usq.edu.au

[2] Canik Basari University, Architecture and Engineering Faculty

Civil Engineering Department, 55080 Samsun, TURKEY

[3] Department of Biological and Agricultural Engineering and Zachry Department of Civil Engineering,

Texas A&M University, 2117 TAMU, College Station, TX 77843-2117, USA

Abstract

Drought forecasting using standardized metrics of rainfall is a core task in hydrology and water resources management. Standardized Precipitation Index (SPI) is a rainfall-based metric that caters for different time-scales at which the drought occurs, and due to its standardization, is well-suited for forecasting drought at different periods in climatically diverse region. This study advances drought modelling using multivariate adaptive regression splines (MARS), least square support vector machine (LSSVM), and M5Tree models by forecasting SPI in eastern Australia. MARS model incorporated rainfall as mandatory predictor with month (periodicity), Southern Oscillation Index, Pacific Decadal Oscillation Index and Indian Ocean Dipole, ENSO Modoki and Nino 3.0, 3.4 and 4.0 data added gradually. The performance was evaluated with root mean square error (*RMSE*), mean absolute error (*MAE*), and coefficient of determination (r^2). Best MARS model required different input combinations, where rainfall, sea surface temperature and periodicity were used for all stations, but ENSO Modoki and Pacific Decadal Oscillation indices were not required for Bathurst, Collarenebri and Yamba, and the Southern Oscillation Index was not required for Collarenebri. Inclusion of periodicity increased the r^2 value by 0.5–8.1% and reduced *RMSE* by 3.0–178.5 %. Comparisons showed that MARS superseded the performance of the other counterparts for three out of five stations with lower *MAE* by 15.0–73.9% and 7.3–42.2%, respectively. For the other stations, M5Tree was better than MARS/LSSVM with lower *MAE* by 13.8–13.4% and 25.7–52.2%, respectively, and for Bathurst, LSSVM yielded more accurate result. For droughts identified by SPI ≤ -0.5, accurate forecasts were attained by

MARS/M5Tree for Bathurst, Yamba and Peak Hill, whereas for Collarenebri and Barraba, M5Tree was better than LSSVM/MARS. Seasonal analysis revealed disparate results where MARS/M5Tree was better than LSSVM. The results highlight the importance of periodicity in drought forecasting and also ascertains that model accuracy scales with geographic/seasonal factors due to complexity of drought and its relationship with inputs and data attributes that can affect the evolution of drought events.

Keywords Standardized precipitation index, drought forecasting, multivariate adaptive regression spline, least square support vector machine, M5 Tree model

1.0 Introduction

Drought is an insidious natural hazard that occurs as a normal, yet a recurrent feature in an arid, semi-arid, desert or rain-forested region (Wilhite et al., 2000a; Keyantash and Dracup, 2002; Vicente-Serrano, 2016). Drought impacts are exacerbated by shifts to warmer and drier conditions, leading to increased water demand compounded by population growth and consequent expansion of industrial, agricultural and energy sectors (McAlpine et al., 2009; IPCC, 2012). As a critical environmental issue, challenges posed by drought elicit increased alertness among hydrologists, agriculturalists and resource planners in strategic decision-making (Bates et al., 2008; Mishra and Singh, 2011). Meteorological drought that transforms in a hydrological, agricultural and socio-economic events, onsets with a marked reduction in rainfall sufficient to trigger hydrometeorological imbalance for a prolonged period (Wilhite and Hayes, 1998; Mishra and Singh, 2010; Deo et al., 2016a). Drought is a costly hazard on socio-economic dimension, occurring on a year-to-year and season-to-season basis with detrimental outcomes due to its persistent effect on groundwater reservoirs, leading to water scarcity, crop failure, disturbed habitats and loss of social/recreational opportunities (Riebsame et al., 1991; Wilhite et al., 2000a; Mpelasoka et al., 2008). Effective strategies to forewarn drought are thus important for risk management.

Effective mitigation and relief strategy for requires a careful consideration of pertinent models to provide quantitative data on future drought (Wilhite and Hayes, 1998; Wilhite et al., 2000a; UN/ISDR, 2007; Şen, 2015). Despite the complexities associated with the understanding of drought itself, perhaps no other natural hazard lends itself quite as much to being able, to predict its progression, given its slow onset where rainfall, evapotranspiration and ground water data can be monitored ahead of time (Cancelliere et al., 2007; UN/ISDR, 2007). Drought monitoring is achieved by studying future changes in drought indices with historical and current

hydrological data (Stahl and van Lanen, 2014; Joaquín Andreu et al., 2015; Deo et al., 2016a). However, an understanding of future drought requires an evaluation of predictive models that are reliable enough to forewarn drought possibility (Mishra and Singh, 2011). Construction of a forewarning systems require action-oriented models that are implemented in a risk management program (Wilhite et al., 2000b; IPCC, 2007; Sheffield and Wood, 2008; Mishra and Singh, 2011).

Due to the complexity of drought that embeds localised, yet stochastic features and non-linearities between predictors and objective variable, modellers remain puzzled in adopting a model for all regions. Spiralling nature of drought makes it impossible to adopt a 'one-size-fits-it-all' so a deficiency in drought mitigation arises from inability to forecast the conditions well in advance (Mishra and Desai, 2005; Almedeij, 2015). Critical issues in drought modelling are: the inability to adopt a universal model, input selection, choice of index that sufficiently represents drought monitoring over different regions and the disproportionally areal and geographic impact that results in different model accuracy (Mishra and Desai, 2005; IPCC, 2012). In some regions, a model may not reflect the reality, thus, a rigorous testing of different models must be facilitated to establish a versatile framework that fits a prediction system. As drought evolves from meteorological to hydrological to agricultural to socio-economic dimensions (Wilhite et al., 2000b; Mpelasoka et al., 2008), the response of a predictive model also varies by the region and timescale, as does the need to select different predictors that best align with the model (Joaquín Andreu et al., 2015). A comparison of different approaches is a paramount task for achieving a robust forecasting model.

According to Lincoln Declaration by World Meteorological Organization (Hayes et al., 2011), Standardized Precipitation Index (SPI) (McKee et al., 1993) was embraced globally as a drought monitoring index. In addition to other region-specific indices, SPI was profusely adopted by National Meteorological and Hydrological Services to characterize meteorological droughts (McKee et al., 1993; Hayes et al., 1999; Yuan and Zhou, 2004; Cancelliere et al., 2007; Svoboda et al., 2012; Jalalkamali et al., 2015; Choubin et al., 2016). SPI is a powerful, yet, a simple and enigmatic-free index that analyses water scarcity situations based on a statistical distribution of rainfall for an aggregation length from one to 48 months. A normalized metric is generated in terms of the standard deviation of rainfall relative to the climatology (McKee et al., 1993; Hayes et al., 1999; Yuan and Zhou, 2004). Due to the normalization of rainfall surpluses/ deficits, SPI model can be applied to investigate drought possibility in climatologically diverse regions (Svoboda et al., 2012; Almedeij, 2015; Choubin et al., 2016). SPI has the ability to describe short and long-term drought at different time scales in a probabilistic manner that makes

it possible to monitor soil moisture conditions that respond to precipitation anomalies on a relatively short timescale, and hydrological reservoirs that reflect long-term rainfall anomalies (Svoboda et al., 2012). SPI is thus an ideal metric for management of not only hydrological but also agricultural drought events (Guttman, 1999).

Drought forecasting based on SPI and data-driven models where drought indicators are used for forecasting, has been researched attentively in different geographic locations. Cancelliere *et al*. (2007) designed an SPI-based methodology for computing drought transition probabilities for Sicily (Italy). Jalalkamali *et al*. (2015) compared a multilayer perceptron artificial neural network (MLP ANN), adaptive neuro-fuzzy inference systems (ANFIS), support vector machine (SVM), and autoregressive integrated moving average (ARIMAX) multivariate model to forecast SPI for Yazd (Iran). Shirmohammadi et al. (2013) used ANFIS, ANN, Wavelet-ANN and Wavelet-ANFIS model for forecasting SPI for Azerbaijan (Iran). Santos *et al*. (2009) generated SPI-based forecasts using ANN for San Francisco and Marj and Meijerin (2011) incorporated satellite-based images and climate indices in ANN to demonstrate drought predictions using North Atlantic and Southern Oscillation Index. Cancelliere *et al*. (2006) employed a non-parametric method to forecast SPI for Sicily and Belayneh and Adamowski (2012) compared ANN, SVR and wavelet neural network models for SPI forecasting in Awash River (Ethiopia). Choubin et al. (2016) developed SPI forecasts by ANFIS, M5 model tree (M5Tree) and an MLP algorithm.

In eastern Australia where this study is focussed, there are synergetic pressures and environmental stress driven by climate shift to warmer temperature, exacerbated by strong El Nino with frequent to severe droughts (McAlpine et al., 2007; Deo et al., 2009; McAlpine et al., 2009; Verdon-Kidd and Kiem, 2009). Drought has become hotter since 1973 with 2002/03 event being >1.0 degree hotter than previous droughts (Nicholls, 2004). Drought poses consequences for runoff that reduces stream flow in agriculturally-sensitive Murray Darling Basin (Cai and Cowan, 2008) with significant economic costs (Wittwer et al., 2002; Dijk et al., 2013). Thus, accurate models can assist with the management of risk and promote economic returns (Timbal and Hendon, 2011; Koehn, 2015; Williams et al., 2015; Qureshi et al., 2016). Consequently, drought has been forecasted using many approaches, for example, with hydrological models (Brown et al., 2015), Markov chain (Rahmat et al., 2016), Bayesian space–time models (Crimp et al., 2015) and recently, data-driven models (Abbot and Marohasy, 2012, 2014; Deo and Şahin, 2015b, a, 2016; Deo et al., 2016b). Notwithstanding this, other than Rahmat et al. (2016) who applied a Markov chain model for SPI modelling, to the best of our

knowledge, there is not any published work on SPI modelling for this important socio-economic region.

Considering the foresaid, this paper illuminates the use of multivariate adaptive regression spline (MARS), least square support vector machine (LSSVM) and M5Tree models for SPI forecasting in drought-prone region of eastern Australia using predictors for five meteorological sites (Figure 3). Except for the far-eastern (Yamba) station, all other sites are situated in Murray Darling Basin that hubs Australia's agricultural belt. The purpose of this paper is threefold. (I) To determine best variables for drought forecasting and test the relative contribution of input variables applied as predictors for the future evolution of SPI. (II) To elucidate the importance of periodicity in drought models and seasonal behaviour of drought. (III) To compare the performances of data-driven models using MARS, LSSVM and M5Tree algoirthms for SPI-forecasting.

2.0 Theoretical Overview

2.1 Multivariate Adaptive Regressions Spline

Introduced by Freidman (1991), MARS has previously been applied hydrology (Abraham and Steinberg, 2001; Sharda et al., 2008; Cheng and Cao, 2014; Deo et al., 2015; Kisi, 2015; Waseem et al., 2015) but its application for SPI forecasting is yet to be undertaken. MARS has an ability to analyze the contributions of each input where interactive effects from exploratory terms are utilized to model the predictand (Cheng and Cao, 2014). It explores complex and non-linear relationships between response and objective variable (Deo et al., 2015) without assumptions on the relationships between inputs and objective variable (Friedman, 1991; Butte et al., 2010). Instead, MARS generates forecasts based on learned relationships from training data partitioned into splines over an equivalent interval (Friedman, 1991). For each spline, inputs, x, are split into subgroups and knots so that they are located between the x and the interval in the same x to separate the subgroups (Friedman, 1991; Sephton, 2001). The knots are 3–4 times the number of basis functions (Sharda et al., 2008) but this limit is deduced by a trial-and-error to avoid over-fitting using shortest distance between neighboring knots (Sephton, 2001; Adamowski et al., 2012).

Fig. 1a shows a schematic view of MARS. In this study MARS utilizes predictors, $\boldsymbol{X}$ defined by [P, SOI, EMI, IOD, PDO, Nino3.0SST, Nino3.4SST and Nino4.0SST] whose time-series evolution are intrinsically related to drought patterns in the objective variable, $\boldsymbol{Y}$ ($\equiv SPI$). First, basis functions, $BF(x)$ are determined and, second, they are projected on the objective vector (Sharda et al., 2008). Suppose $\boldsymbol{X}$ is the vector (x_1, $x_2 \ldots x_N$),

$$\mathbf{Y} = g(\mathbf{X}) + \xi \tag{1}$$

where ξ is the distribution of model error (Deo et al., 2015; Kisi, 2015) and N is the number of training data points.

MARS approximates $g(.)$ by applying respective $BF(x)$ with piecewise linear functions: max $(0, x - c)$ where a knot occurs at the position c (Zhang and Goh, 2013). The equation max (.) means that only the positive part of (.) is used, otherwise it will be given a zero value concordant with:

$$\max(0, x-c) = \begin{cases} x-c, & if\ c \geq t \\ 0, & otherwise \end{cases} \tag{2}$$

Thus, $g(\mathbf{X})$ is constructed as a linear combination of $BF(x)$:

$$g(\mathbf{X}) = \beta_o + \sum_{n=1}^{N} \beta_n BF(\mathbf{X}) \tag{3}$$

where β is a constant estimated using the least-square method.

As MARS is data-driven, $g(\mathbf{X})$ is applied in a forward-backward stepwise method to input data to identify the location of the knots where the function value is found to vary (Adamowski and Karapataki, 2010). At the end of the forward phase, a large model which, in fact, may over-fit the trained input data is achieved so a backward deletion phase is engaged where the model is simplified by deleting one least basis function according to the Generalized Cross Validation, GCV, as a form of regularisation, is given by (Craven and Wahba, 1978):

$$GCV = \frac{MSE}{\left[1 - \frac{CM}{N}\right]^2} \tag{4}$$

where MSE is mean squared error of the evaluated model and CM is the penalty factor:

$$CM = M + dM \tag{5}$$

Eq. (5) estimates how well the MARS model performs on new (forecasted) data (Deo et al., 2015). If several basis functions are chosen, an over-fitting can occur so some basis functions are deleted in the pruning phase (Samui, 2012; Kisi, 2015) to select the "best" model with the lowest GCV.

< Fig. 1a-c>

2.1 M5Model Tree

M5Model Tree, introduced by Quinlan (1992), is a hierarchical model based on binary decision framework. It utilizes linear regressions at terminal (leaf) nodes that develop relationships

between inputs/output variable (Mitchell, 1997). A dual stage process is applied for constructing an M5Tree (Rahimikhoob et al., 2013) where input/output data are split in subsets to create a decision tree. Consider *N*-sample training matrices characterized by (input) patterns/attributes associated with a predictand. M5Tree constructs a model relating a target value of training case to the input attributes (Bhattacharya and Solomatine, 2005). In context of drought modelling, M5Tree maps the relationships between inputs and *SPI* based on matched attributes. Fig. 1b shows a schematic view of the M5Model Tree.

Using 'divide-and-conquer', a model is constructed where *N* points are associated with a leaf or a test criterion that splits them into subsets corresponding to a test outcome. This process is applied recursively where subsets created from *N* points follow a criterion depending on the standard deviation of class values and calculating the reduction in error, σ_R (Bhattacharya and Solomatine, 2005; Kisi, 2015):

$$\sigma_R = \sigma(\Lambda) - \sum\left(\frac{\Lambda_i}{\Lambda}\sigma(\Lambda_i)\right) \tag{6}$$

where Λ is a set of examples that reach the node and Λ_i is the subset of examples that have the i^{th} outcome of the potential set.

When maximum splits (including patterns/attributes and splits) are attained, M5Tree selects them to maximize σ_R to select a model with the lowest σ_R. Splitting ceases when the class value of all instances reaching a node do not vary or that just a few instances remain. It so turns out that the perpetual division rule applied to input data can lead to very large, over-elaborate network of structures that must be pruned back. If a model is constructed from a smaller number of training points, a smoothing process needs to be applied to compensate for the abrupt discontinuities that can occur between adjacent linear models at the leaves of the pruned tree (Bhattacharya and Solomatine, 2005; Kisi, 2015). This improves the accuracy of the fine-tuned model. During the smoothing, the linear equations are updated so that the forecasted output for the input vectors corresponding to different equations become close to each other. For detailed discussion on M5Tree, readers can refer to Quinlan (1992) and Witten and Frank (2005).

2.3 Least Square Support Vector Machine

LSSVM is based on structural risk minimization (Vapnik and Vapnik, 1998) with a regularization constraint on the model's weight. It alleviates convex quadratic programming associated with support vector machines (SVM) (Suykens et al., 1999; Suykens and Vandewalle, 1999). In SVM, "slackness" is set by an inequality constraint. However, LSSVM avoids this

(and solves the regression problem as a set of linear equations). This is an advantage, as it can provide faster training and higher stability and accuracy (Sadri and Burn, 2012). It yields global solutions to error function that it minimizes, exhibiting merits over gradient based models (e.g. artificial neural network) (Bishop, 1995; Cherkassky and Mulier, 2007). In LSSVM, a kernel function (*K*) and its parameters are optimised so that a bound on Vapnik–Chervonenkis dimension is minimized to yield stable solutions (Müller et al., 1997).

If ***X*** is a time-series (x_1, x_2… x_N) and intakes any training variable: (*P*, SOI, EMI, IOD, PDO, Nino3.0SST, Nino3.4SST and Nino4.0SST), and ***Y*** (≡ *SPI*) is the objective variable, the LSSVM model is:

$$\mathbf{Y}(\mathbf{X}) = f(\mathbf{B}) = w^T \Psi(\mathbf{X}) + \mathrm{B} \tag{7}$$

where *w*, ψ and B = weight vectors, mapping functions and bias terms, respectively (Suykens et al., 1999; Suykens et al., 2002).

Based on the function's estimation error, the LSSVM model is normally designed using structural risk minimisation applied to the *J* term, written as:

$$\min J(w,e) = \frac{1}{2} w^T w + \frac{C}{2} \sum_{i=1}^{m} e_i^2 \tag{8}$$

where e_i^2 is the quadratic loss term, *W* is the weight vector, and *C* is the cost (or regularization) parameter (a positive constant).

Eq. (8) is subject to the following constraint (Kisi, 2015):

$$y_i = w^T \Psi(x_i) + \mathrm{B} + e_i \quad (i = 1, 2, ..., m) \tag{9}$$

To solve for the model parameters, a Lagrangian multiplier ($\alpha_i \in R^N$) is adopted (Kisi, 2015):

$$\Gamma(w, \mathrm{B}, e, C) = J(w, e) - \sum_{i=1}^{m} \alpha_i \left\{ w^T \Psi(x_i) + b + e_i - y_i \right\} \tag{9}$$

The conditions which prove optimal in solving the parameters are determined by taking the partial-derivatives of the extended loss function (i.e. $\Gamma(W, B, e, \alpha)$) with respect to each term (i.e. *W*, *B*, *e*, α) (Kisi, 2015):

$$\begin{cases} w = \sum_{i=1}^{m} \alpha_i \Psi(x_i) \\ \sum_{i=1}^{m} \alpha_i = 0 \\ \alpha_i = Ce_i \\ w^T \Psi(x_i) + \mathrm{B} + e_i - y_i = 0 \end{cases} \tag{11}$$

where $\psi(x)$ is a nonlinear mapping function related to kernel function.

In matrix form, these are expressed as (Suykens et al., 1999):

$$\begin{bmatrix} 0 & -Y^T \\ Y\ \Omega\Omega^T + \dfrac{I}{C} \end{bmatrix} \begin{bmatrix} \mathrm{B} \\ \alpha \end{bmatrix} = \begin{bmatrix} 0 \\ I \end{bmatrix} \tag{12}$$

where $Y = \{y_1, \ldots, y_m\}, \Omega = \Psi(x_1)^T y_1, \ldots, \Psi(x_m)^T y_m, I = \{1, \ldots, 1\}, \alpha = \{\alpha_1, \ldots, \alpha_l\}$.

Note that Ω is used to represent the kernel function satisfies Mercer's theorem (Okkan and Serbes, 2012). Finally, LSSVM model is expressed as:

$$f(x) = \sum_{i=1}^{m} \alpha_i \Omega(x, x_i) + \mathrm{B} \tag{13}$$

In this study we applied the radial basis kernel function (RBF):

$$\Omega(x, x_i) = \exp\left(\frac{-\|x - x_i\|^2}{2\sigma^2} \right) \tag{14}$$

Here, the σ as the kernel width. Both the C and σ are determined by a grid search process (Goyal et al., 2014; Deo et al., 2016b; Deo et al., 2016c).

2.4 Standardized Precipitation Index

In order to develop a drought forecasting model for the study region, the monthly Standardized Precipitation Index (SPI) was first computed following McKee *et al*. (1993). In general, computing SPI involves fitting the gamma probability density function to the given distribution of monthly rainfall (P) data. The gamma distribution function is defined by its probability density function, $g(P)$:

$$g(P) = \frac{1}{\beta^{\alpha}\Gamma(\alpha)} P^{\alpha-1} e^{-x/\beta} \tag{15}$$

where parameters, α and β, can be estimated using the maximum likelihood solution:

$$\alpha = \frac{1}{4A}\left(1+\sqrt{\frac{1+4A}{3}}\right) \tag{16}$$

$$\beta = \frac{\alpha}{\bar{P}} \tag{18}$$

and $A = \ln(\bar{P}) - \left(\sum \ln(P)\right)/N$, and N = the number of rainfall observation months. The cumulative probability can be given by

$$G(P) = \int_0^P g(P)dP = \frac{1}{\beta^{\alpha}\Gamma(\alpha)}\int_0^P x^{\alpha-1}e^{-P/\beta}dP \tag{19}$$

Letting $t = P/\beta$, Eq. (19) becomes an incomplete gamma function:

$$G(P) = \frac{1}{\Gamma(\alpha)}\int_0^t t^{\alpha-1}e^{-t}dt \tag{20}$$

As the gamma function is undefined for $P = 0$, the cumulative probability becomes:

$$H(P) = q + (1-q)\,G(P) \tag{21}$$

where q is the probability of zero. The cumulative probability $H(P)$ can be transformed into the standard normal random variable with mean zero and variance of one. This yields the monthly value of SPI, viz:

$$SPI = \begin{cases} +\left(t - \dfrac{c_0 + c_1 t + c_2 t^2}{1 + d_1 t + d_2 t^2 + d_3 t^3}\right), & 0.5 < H(P) \le 1.0 \\ -\left(t - \dfrac{c_0 + c_1 t + c_2 t^2}{1 + d_1 t + d_2 t^2 + d_3 t^3}\right), & 0 < H(P) \le 0.5 \end{cases} \tag{22}$$

In Eq. (22), t is given by:

$$t = \begin{cases} \sqrt{\ln\left(\dfrac{1}{[H(P)]^2}\right)} & 0 < H(P) \le 0.5 \\ \sqrt{\ln\left(\dfrac{1}{[1.0 - H(P)]^2}\right)} & 0.5 < H(P) \le 1.0 \end{cases} \tag{23}$$

In Eq. (23), the constants are as follows: c_0 = 2.515517, c_1 = 0.802853, c_2 = 0.010328, d_1 = 1.432788, d_2 = 0.189269 and d_3 = 0.001308 (McKee et al., 1993). The 'drought' part of the SPI range can be split into the 'moderately dry' (−1.5 < SPI ≤ 1.0), 'severely dry' (−1.5 ≤ SPI < −2.0), and 'extremely dry' (SPI ≤ −2.0) categories.

< Fig. 2 >

Fig. 2 illustrates a practical applicability of SPI for monitoring the progression of drought using the drought monitoring data for Bathurst Agricultural Station for part of the Millennium Drought event (January 2002 – April 2003). Following the running sum approach of Yevjevich

(1967, 1991), the onset of drought can be taken the month when the SPI value declines below 0 and the termination of drought when the SPI first returns to positivity. Within this drought period that is consistent with a significant reduction in the cumulative monthly rainfall, the duration of drought event can be taken as the sum of all months with SPI < 0 and the peak intensity when the SPI value is at its minimum value.

3.0 Materials and Method

3.1 Study Area and Data

In this study a set of drought forecasting models, based on the SPI time-series, were employed for five meteorological sites (Fig. 3). The sites are located in eastern Australia (state of New South Wales) where drought is a common occurrence and leads to consequences for agricultural activities in the Murray Darling Basin (Deo et al., 2009; Helman, 2009; McAlpine et al., 2009). Table 1 lists the geographical and hydrological statistics for annual data averaged over a period from 1915–2012. The sites depict diverse climatic features with elevations from 29–713 m year^{-1} and mean annual rainfall from 279.77–750.35 mm year^{1} with a standard deviation of 23.93–50.83 mm year^{-1}. The climatologically averaged minimum rainfall is 1.06 mm year^{-1} (Collarenebri) and maximum rainfall is 9.39 mm year^{-1} (Bathurst Agricultural Station). Apart from Yamba Station which is located in the coastal end of eastern Australia, the other stations (Bathurst Agricultural, Collarenebri, Peak Hill, Barraba and Yamba) are situated in Murray Darling Basin. Therefore, drought modelling in this region is considered as a novel task for the management of drought-risk to the agricultural sector.

< Table 1>

< Fig. 3>

A set of models based on MARS, LSSVM and M5Tree algorithm was developed using monthly rainfall (*P*) from 1915–2012. The *P*-data were acquired from Australian Bureau of Meteorology's high quality (HQ) archives (Lavery et al., 1997; BOM, 2008) which had been quality-checked using standard normal homogeneity tests. Accordingly, the recorded rainfall had been adjusted for inhomogeneity caused by external factors, such as station relocations, instrumental errors, and adverse exposure to the measurement site (Alexandersson, 1986; Torok and Nicholls, 1996). The process detects and removes gross single-day errors in data. Rather than making inhomogeneity adjustments in mean values, daily records were adjusted for discontinuities at the 5, 10… 90, 95 percentiles. Missing data were deduced by generating artificial rainfall based on cumulative rainfall distributions (Haylock and Nicholls, 2000).

Consequently these data have since been used for climate studies (Suppiah and Hennessy, 1998; Alexander et al., 2006; Deo and Şahin, 2015b, a; Deo et al., 2016a; Deo et al., 2016b).

As data-driven models rely on predictive features in historical data to forecast future drought, climate indices and sea surface temperature (SST) were used as regression covariates to feed in such attributes and data patterns for the respective drought model. The climate of eastern Australian responds to oceanic phases, defined by the Southern Oscillation Index (SOI), Pacific Decadal Oscillation Index (PDO), Indian Ocean Dipole (IOD) and ENSO Modoki Index (EMI) and Nino 3.0, Nino 3.4 and Nino 4.0 SST (Nicholls, 2004; Helman, 2009; Ummenhofer et al., 2009; Dijk et al., 2013). In earlier studies, the PDO and IOD phases were associated with drought (McKeon et al., 2004; McAlpine et al., 2009), and rainfall and streamflow patterns in central and southern parts of Murray Darling Basin exhibit significant perturbations due to SOI, PDO and IOD phases (Verdon and Franks, 2006; McGowan et al., 2009). When central eastern Pacific region's SST is warm and PDO is in positivity, eastern Australia is generally warm and dry (Jones et al., 1996; Power et al., 1999; Ummenhofer et al., 2009). Similarly, EMI moderates austral autumn rainfall (Ashok et al., 2007; Cai and Cowan, 2009). Considering this, no single index can fully explain how the future drought will evolve (Helman, 2009). Therefore, the study utilised the SOI and IOD data (Australian Bureau of Meteorology) (Trenberth, 1984), PDO (Joint Institute of Study of Atmosphere and Ocean) (Mantua et al., 1997; Zhang et al., 1997), EMI (Japanese Agency for Marine Earth Science and Technology) (Ashok et al., 2007; Weng et al., 2007; Weng et al., 2009), and SST (National Prediction Centre) as the predictor variables for MARS, LSSVM and M5Tree models.

<Table 2>

3.2 Drought Model Development

To validate the potential utility of data-driven algorithms for drought modelling at five study sites in eastern Australia, the drought models were developed using MATLAB software. The predictor variables (x) comprised monthly observations of rainfall, sea surface temperature (Nino 3.0, Nino 3.4 and Nino 4.0 SST), and climate indices (SOI, PDO, IOD and EMI) for the period 1915–2012 (Table 2). The data were partitioned in the 50:25:25 ratios to create the training (01/1915–12/1963) and validation/testing sets (01/1964–12/2012), respectively (Table 3).

<Table 3>

In the case of data-sparse situations, a drought modeller must have the knowledge of the relevant predictors or input(s) to develop a parsimonious forecasting model. As the drought phenomenon is complex and has poorly understood relationships that exist between target (SPI)

and predictor variable (x) (Mishra and Singh, 2010, 2011), determining the appropriate set of inputs to provide an accurate and reliable forecast model is challenging (Abbot and Marohasy, 2014). A useful preliminary step is to examine the individual relationships between x and the target output (i.e. SPI). Therefore, in this study, the cross correlation coefficient, r_{cross}, between objective ($y \equiv$ SPI) and predictor variable (x) in the training period was acquired to check the role of predictor in modelling the drought index. The magnitude of r_{cross} which measures similarity between y and shifted (lagged) copies of $x_i = (x_1, x_2 \ldots x_{M-1})$ and $y = (y_1, y_2 \ldots y_{N-1})$ was given by the covariance:

$$\phi_{xy,k} = \sum_{j=\max(0,k)}^{\min(M-1+k,N-1)} x_{j-k}, \quad k = -(M+1),\ldots,0,\ldots,(N-1) \tag{24.1}$$

$$r_{cross}(t) = \frac{\phi_{xy}(t)}{\sqrt{\phi_{xx}(0)\ \ \phi_{yy}(0)}} \tag{24.2}$$

where $r_{cross}(t)$ is expected to vary between -1 and 1 for any t (lagged timescale). Table 4 shows the cross correlation of inputs (versus *SPI*) where statistically significant correlation at the 95% level of confidence is indicated. The strongest and statistically significant correlation coefficient with $0.833 \le r_{cross} \le 0.897$ is obtained for rainfall as a predictor variable for SPI followed by SOI ($0.211 \le r_{cross} \le 0.247$) and Nino 4.0 SST ($-0.159 \le r_{cross} \le -0.131$). The value of r_{cross} for the case of Nino3.4 SST as a predictor variable was also statistically significant, albeit the strength of correlation was relatively weaker. According to this result, the study utilized rainfall as a mandatory input variable for SPI forecasting.

<Table 4>

In order to develop MARS, the most appropriate basis functions (Eq. 3) were deduced for each study site by developing regression trees to attain the optimal model. For M5Tree model, a tree-based forecasting model was constructed using the 'divide-and-conquer rule' (Rahimikhoob et al., 2013; Kisi, 2015), which was later fine-tuned. An example of regression trees for optimum MARS and M5Tree models for Bathurst Agricultural Station is given in Appendix (Table A1 and A2). For designing the optimum LSSVM model, a grid search procedure (Hsu et al., 2003; Lin and Lin, 2003) was applied to determine the optimum regularisation constant (Eq. 8) and RBF kernel width (Eq. 14). As an example, the variation of root mean square error (RMSE) attained versus the range of regularisation constants and kernel widths tested for Bathurst Agricultural Station is shown in Fig. 3. In accordance with literature (Hsu et al., 2003; Lin and

Lin, 2003; Hsu et al., 2008), it is evident that for a given combination of C and σ, the RMSE value for the model obtained is unique. Thus, for all stations considered, the magnitude of LSSVM model parameters were optimised to reduce model error. The drought models were evaluated according to the agreement between forecasted and observed SPIs within the validation period.

<Fig. 3>

3.3 Model Evaluation Criteria

In the model evaluation phase, one must not rely on a single statistical metric but rather should utilise a range of performance indicators to validate the drought modelling skills from different perspectives (Krause et al., 2005; Dawson et al., 2007). In this study, the accuracy of MARS, LSSVM and M5Tree was evaluated primarily using the root mean square error (*RMSE*), mean absolute error (*MAE*) and coefficient of determination (r^2) (Krause et al., 2005), viz:

$$RMSE = \sqrt{\frac{1}{N}\sum_{i=1}^{N}\left(SPI_{i,o} - SPI_{i,f}\right)^2} \tag{25}$$

$$MAE = \frac{1}{N}\sum_{i=1}^{N}\left|SPI_{i,o} - SPI_{i,f}\right| \tag{26}$$

$$r^2 = \left(\frac{\sum_{i=1}^{N}\left(SPI_{i,o} - \overline{SPI}_o\right)\left(SPI_{i,f} - \overline{SPI}_f\right)}{\sqrt{\sum_{i=1}^{N}\left(SPI_{i,o} - \overline{SPI}_o\right)^2}\sqrt{\sum_{i=1}^{N} SPI_{i,f} - \overline{SPI}_f} } \right)^2 , -1 \le R^2 \le 1 \tag{27}$$

where N (=294) was the number of test samples, SPI_o and SPI_f were the i^{th} value of the observed and forecasted SPIs in validation/testing period.

As a widely adopted model evaluation metric, *RMSE* and *MAE* were able to assess the forecasting capability of the data-driven models where *RMSE* deduced the goodness-of-fit relevant to high SPI values, whereas *MAE* was not weighted towards high(er) magnitude or low(er) magnitude events, but instead evaluated all deviations of forecasts from the observed values, in an equal manner and regardless of sign (Deo et al., 2016b). It should be noted that r^2, which was bounded by [-1, 1], described the proportion of statistical variance in the observed values of SPI that was explained by the drought forecasting model. The equation, however, was based on a consideration of linear relationship between SPI_f and SPI_i and was, therefore, limited, as it standardized to the observed and modelled values of mean and variance (Deo et al., 2016b).

In this study, drought models were developed and tested for geographically diverse sites in eastern Australia that exhibit different climatic patterns. To compare results for different sites, the normalised form of *MAE*, represented as the percentage inaccuracy of the forecasted relative to the observed SPI, was computed viz:

$$MAPE = \frac{1}{N}\sum_{i=1}^{N}\left|\left(\frac{SPI_{i,f} - SPI_{i,o}}{SPI_{i,o}}\right)\right| \times 100\,, \quad 0 \le MAPE \le 100 \tag{28}$$

The Willmott's Index (*WI*), which in fact resolves the potential bias issues in *RMSE*, was also determined (Willmott, 1981; Krause et al., 2005):

$$WI = 1 - \left[\frac{\sum_{i=1}^{N}\left(SPI_{i,o} - SPI_{i,p}\right)^2}{\sum_{i=1}^{N}\left(\left|SPI_{i,p} - \overline{SPI}_{i,o}\right| + \left|SPI_{i,o} - \overline{SPI}_{i,o}\right|\right)^2}\right], 0 \le d \le 1 \tag{29}$$

It is noteworthy that the *WI* is advantageous over the *RMSE* and the R^2 value where the differences in monthly SPI from observed and forecasted data are described as squared values, hence larger values of the forecasted SPI are overestimated, whereas smaller values are neglected (Legates and McCabe, 1999). However, *WI* was able to overcome this insensitivity of model error (Willmott, 1981), as the ratio of mean square error is considered rather than the square of the error differences (Willmott, 1984).

4.0 Results and Discussion

In this section, results attained from MARS, LSSVM and M5Tree for forecasting monthly SPI in eastern Australia are assessed to validate their adequacy in drought modelling study. The SPI forecasted using MARS was analysed where the importance of input variables was checked in terms of the predictive accuracy. Then, MARS, LSSVM and M5Tree were compared, based on statistical performance criteria (Eq. 25–29), including a seasonal analysis of model accuracy.

Table 5 shows the forecasting accuracy of MARS in training, validation and testing periods with a single input variable (rainfall) and gradually added inputs (with climate indices and sea surface temperature) as the supplementary predictor variables. Although rainfall data were utilised as the mandatory input variable subject to highest cross correlation with observed SPI (e.g. Table 4), the order of the other input combinations was not decided upon *apriori* but rather how the MARS model responded to the forecasted value of SPI in the training, validation and testing periods. Accordingly, the magnitude of *RMSE*, *MAE* and R^2 between forecasted and

observed SPIs were examined for each site and the respective input combinations to generate a total of nine modelling scenarios (M1–M9) (see Table 5).

<Table 5>

According to the results presented in the testing period, a significant dependence of the model accuracy on the geographic distribution of stations was demonstrated where different input combinations were necessary for attaining the most accurate predictive model. Consider, for example, the case of Bathurst Agricultural Station; the MARS model utilised rainfall, all of the three SSTs data, SOI and the month to yield the lowest value of *RMSE*/*MAE* and the highest R^2 value of approximately 0.159, 0.159 and 0.976, respectively, whereas for Collarenebri, the most accurate result was attained without SOI as a predictor variable (Table 5a). A closer examination of this result also showed that if redundant variables were included in the MARS model, the performance either remained stationary or declined for some study sites. This was true for the case of the Bathurst Agricultural Station, where the model M5 exhibited a value of R^2 = 0.957 and *RMSE/MAE* = 0.222/0.174 with rainfall, SSTs and SOI as the predictor variables, but the inclusion of PDO, IOD and EMI did not improve the model's forecasting accuracy.

<Fig. 5>

It is important to note that an inclusion of the month (that indicates periodicity) as a predictor variable for all five stations led to a marked improvement in the MARS model's performance. This has also been illustrated in Fig. 5 with a scatterplot of the forecasted value of SPI (SPI_F) relative to the observed (SPI_O) in the testing period. In accordance with this, the degree of scatter was reduced and the correspondence of linear agreement between SPI_F and SPI_O was improved for all test stations. Consistently, the r^2 value was also increased by about 2.0% and *RMSE* was decreased by about 28.4% for Bathurst Agricultural Station. A similar deduction was made for Collarenebri station, where virtually no improvement was noted in the models denoted as M5, M6 and M7 relative to the model denoted as M4 when SOI, PDO and IOD were included as predictor variables (Table 5b). In fact, for the Yamba station, there was a dramatic improvement in the accuracy of M5 relative to M1, M2, M3 and M4, with *RMSE* of about 0.298 compared to 0.304, 0.335, 0.346 and 0.358, respectively. However, when the time series of PDO, IOD and EMI were added gradually into the models M6, M7 and M8, respectively, the *RMSE* value increased from 0.302–0.314 and the r^2 value decreased from 0.910–0.896. On the other hand, the exclusion of PDO, IOD and EMI as the model inputs led to a marked improvement in the overall performance, with a reduction in *RMSE* by 64.1% and an increase in r^2 by 9.1% (Table 5e). This result was consistent with other studies (e.g. (Lyon et al., 2012)), where the SPI prediction was improved by using seasonality as a predictor variable.

While it is unambiguous that the optimum MARS model for Bathurst Agricultural Station, and Collarenebri and Yamba stations did not require the PDO, IOD and EMI data as input variables, the forecasted results for Peak Hill and Barraba stations were in fact significantly dependent on these data (including SOI) as a predictor variable (Table 4c-d). Despite a certain degree of variation in terms of how each of the input variables acts to moderate the r^2 and *RMSE*/*MAE* values, an overall improvement in model performance was evident when all nine predictor variables for Peak Hill and the eight predictor variables for Barraba station were incorporated in the MARS model. Clearly, this indicated that the optimum MARS model responded quite differently to the different input variables used as predictors (Table 5). Likewise, the accuracy of the MARS model exhibited a significant variability in its overall performance based on the geographic distribution of the present study sites (Fig. 2). It is noteworthy that the role of periodicity in drought forecasting was clearly demonstrated by the MARS model, where an improvement in performance was evident for the sites with month as a predictor variable.

<Fig. 6>

In Fig. 6 the forecasting error, $E = SPI_F - SPI_O$, deduced in the last five years of testing data for MARS, LSSVM and M5Tree models is shown, where the month (periodicity) was utlilised as a predictor variable in addition to the other variabales (Table 2). To also demonstrate the model's statistical performance with and without periodicity, Table 6 compares the results for MARS, M5Tree and LSSVM models with only the optimum input combinations. In terms of the agreement between observed and forecasted SPIs for the best model, the time-series plot of error values depicted the MARS and M5Tree models as being more accurate than the LSSVM model, especially for Bathurst Agricultural Station, and Collarenebri and Yamba stations, where the amplitudes of *E* were generally smaller for majority of the test points. However, when *RMSE*, *MABE* and r^2 values were compared in the testing period (Table 6), the MARS model performed better (*RMSE* = 0.132, r^2 = 0.980) than the other two counterparts for the case of Peak Hill and Yamba stations, whereas the M5Tree model yielded better performance for the case of Collarenebri and Barraba stations (*RMSE* = 0.174, r^2 = 0.971 and *RMSE* = 0.179, r^2 = 0.974, respectively). For the case of Bathurst Agricultural Station, LSSVM produced modestly better forecasts (*RMSE* = 0.159, *MAE* = 0.109, r^2= 0.977) than the MARS (*RMSE* = 0.159, *MAE* = 0.150, r^2= 0.976) and M5Tree ((*RMSE* = 0.244, *MAE* = 0.150, r^2= 0.948) models. Consistent with the MARS model (Table 5; Fig. 6), for all stations considered the LSSVM and M5Tree models also yielded significantly better results where periodicity was utilized as a predictor variable.

<Table 7>

As the geographic locations of study sites are diverse (Fig. 2), as also stipulated by distinct hydrological conditions (Table 1), comparison of the relative forecasting errors should be made in order to assess the model's accuracy for one site relative to another (Krause et al., 2005; Dawson et al., 2007; Deo et al., 2016c). Thus, Willmott's index of agreement (*WI*) and the mean absolute percentage error (*MAPE*) (%) deduced in accordance with Eq. 28 and 29 for the MARS, LSSVM and M5Tree models were made. Table 7 lists the values of *WI* and *MAPE*. For the case of Bathurst Agricultural Station, it was interesting to note that in contrast to the conclusion reached on the basis of *RMSE*, *MAE* and r^2 where LSSVM was better than MARS and M5Tree models (Table 6), the model evaluation based on *WI* and *MAPE* suggested that the MARS model was more accurate (*WI* = 0.989, *MAPE* = 29.05%) than LSSVM and M5Tree (0.988, 34.164% and 0.977, 50.86%, respectively) (Table 7). However, without ignoring the fact that the differences between MARS and LSSVM was marginal (Table 6), it can be construed that both MARS and LSSVM models appear to be suitable for SPI-based forecasting Bathurst Agricultural Station.

For the cases of Peak Hill and Yamba stations, the *MAPE* and *WI* clearly stipulate the superiority of MARS over LSSVM and M5Tree models. When the values of *MAPE* and *WI* were evaluated for the case of Collarenebri and Barraba stations, the results in Table 7 revealed a dramatically better performance of M5Tree with MARS and LSSVM models being significantly erroneous. That is, the magnitude of *MAPE* was approximately 46.77 and 39.18% (for Collarenebri) and 43.833 and 79.30% (for Barraba) relative to 29.098 and 37.94% generated by the M5Tree model. This indicated that an SPI-based drought forecasting model using M5Tree model should preferentially be adopted over the MARS and LSSVM models. However, the M5Tree model should incorporate the monthly cycle as a predictor variable so that the drought evolution over time is considered to yield more accurate and reliable forecasting performance.

<Fig. 7>

In Figure 7 the frequency distribution of MARS, LSSVM and M5Tree model's forecasting error in an increment of 0.10 has been shown where the percentage of the months in the test period with an error magnitude of ±0.10 has been collated. It was evident that the frequency of forecasting errors yielded by the MARS model within the smallest error bracket (±0.10) was recorded to be the highest for the case of Bathurst Agricultural Station (≈62.6%) and Yamba (≈76.9%) station. This indicated the superiority of MARS over LSSVM and M5Tree models. On the other hand, for the case of Collarenebri, Peak Hill and Barraba stations, the M5Tree model was seen to perform with greater accuracy when the cumulative percentages of model errors in the smallest error bracket were evaluated. Although this result appeared to

accede the deduction made according to the mean absolute percentage error for Collarenebri and Barraba (Table 7), it contrasted the results for Peak Hill station where the *MAPE* value was the lowest for the MARS model. This showed that although the overall performance with the MARS model was better for Peak Hill, the MARS model could produce a majority of the forecasting errors in the test period with small error magnitudes (Fig. 7).

<Table 8>

So far, an evaluation of the prescribed data-driven models was restricted to the assessment of the forecasted and observed SPI values in the entire test dataset (1998–2012), including the cases of negative SPI (dry condition) and positive SPI (wet condition). However, in real-time drought forecasting, it is vital to clearly establish whether the prescribed MARS, LSSVM and M5Tree models are accurate enough to be able to simulate the drought segment of the SPI, as such information is more useful for drought-risk and water resources management. The exclusion of non-drought part of SPI for drought model assessment is also important as it provides the modeler crucial information on whether the model is able to represent future drought cases adequately. Table 8 shows a closer analysis of forecasting results of the drought part of SPI within the test period, where the relative forecasting error (%) in respect of the observed SPI $\leq$ -2.0 (extreme drought), -1.5 $\leq$ SPI < -2.0 (severe drought) and -0.5 $\leq$ SPI < 1.5 (moderate drought) is summarized.

It is evidenced that M5Tree and MARS were highly accurate, compared to the LSSVM model for all study sites considered as well as the different category of drought events that were forecasted (Table 8). Considering the case of forecasting moderate drought events (Table 8a), the M5Tree model yielded a relative error of between 5.90–13.6% for at least four (Collarenebri, Peak Hill, Barraba and Yamba) out of five stations, whereas the MARS and LSSVM models yielded errors of 10.9–17.7%, and 16.5–19.3%, respectively. Similarly, for severe drought forecasting, the M5Tree model was dramatically better with the relative errors of about 3.0–5.2% for at least three stations (i.e. Collarenebri, Peak Hill and Barraba) than with 5.9–21.2% (MARS) and 11.4–27.1% (LSSVM) models. Likewise, for extreme drought forecasting, the M5Tree model was better than LSSVM and MARS, with relative errors of 4.9–11.8% for Bathurst, Collarenebri, Barraba and Yamba compared with about 9.1–30.9% (MARS) and 16.0–37.2% (LSSVM). It is imperative to note that the LSSVM model generated the largest magnitude of forecasting error for all five stations tested within the severe and extreme drought categories (*MAPE* = 7.6–30.6% and 16.0–37.2%, respectively). The results thus indicate that the LSSVM model was unsuitable for modelling drought events in the study area.

While M5Tree was found to be relatively superior to the MARS and LSSVM models for a majority of the sites, there appeared to be a significant dependence of the respective model performance on the geographic distribution of sites. For example, in the case of extreme drought forecasts, M5Tree was more accurate than MARS for all sites except Peak Hill. In fact, for the latter station, MARS outperformed the M5Tree model, where relative forecasting errors of ≈0.20% compared with 4.9% (M5Tree) and 37.2% (LSSVM) were recorded (Table 8a). The model developed for severe and moderate drought forecasting found M5Tree as being more accurate than MARS when tested for Collarenebri, Barraba and Yamba stations (*MAPE* ≈ 3.0–5.2%) compared to 6.6% and 1.3% for Bathurst and Yamba stations (Table 8b). Accordingly, it can be concluded that the drought models exhibited a strong geographic behavior in their accuracy, which shows the complexity of drought behavior and the different data attributes and patterns in the predictor variables used to forecast SPI. Notwithstanding this, it is perceived that while MARS exhibited an overall better performance for a number of stations when evaluated for the entire test data (Tables 6 and 7), the M5Tree model resulted in much better accuracy when the drought segment of the test signal was analyzed (Table 8).

By an analysis of the monthly values of the forecasted and observed SPI data, the model errors generated by MARS, M5Tree and LSSVR over different seasons were also checked in the austral summer (December-January-February), autumn (March-April-May), winter (June-July-August) and spring (September-October-November) periods (Table 9). Results showed that the MARS and M5Tree models were generally more accurate in SPI forecasting than the LSSVM model. In fact, for the Collarenebri station, M5Tree exhibited the lowest value of *MAPE* for all four seasons and for Barraba, the model errors were the smallest for the DJF, MAM and SON periods. For the JJA period, the M5Tree model yielded an error whose magnitude was very close to that of the MARS model (29.5% compared to 29.2%). This showed that for Collarenebri and Barraba stations, M5Tree was more appropriate for drought modelling over the LSSVM and MARS models. Whereas the relative seasonal errors generated by the M5Tree model for Yamba station were approximately 42.19–37.78% lower than those of the MARS model for DJF and SON seasons, the error for MAM and JJA periods was approximately 15.05–75.75% larger. It was noteworthy that for Bathurst Agricultural Station, the MARS model was the most accurate model for SPI forecasting. Interestingly, except for the SON season for Bathurst Agricultural Station, the forecasted and observed values of SPI generated by LSSVM had a very poor agreement for all study sites, as confirmed by the elevated values of *MABE*. This was consistent with earlier results (Table 6, 7 & 8; Figures 4, 6 & 7) by means of statistical and visual agreements between the values of SPI_F and those of SPI_O.

Table 9>

5.0 Further Discussion, Limitations and Future Work

The results acquired for modelling monthly SPI using the MARS, LSSVM and M5Tree algorithms highlighted a pivotal role of periodicity as a crucial driver of model accuracy, among other predictors in order of their relative importance. This was clearly evident by the improved performance of models with monthly cycle as an input, which yielded lower *RMSE*, *MAE* and larger r^2 (Tables 5 and 6) compared to the forecasts without applying the periodicity factor. These results also resonate with those of other investigations (e.g. (Kane and Trivedi, 1986; Kane, 1997; Almedeij, 2015; Moreira et al., 2015)), where periodicity in the drought behavior was found to be associated with the seasonality of input variables and the respective phases of atmospheric-oceanic oscillation, such as the quasi-biennial oscillation (QBO), solar activity, ENSO, Inter-decadal Pacific Oscillation (IPO) and intensification of subtropical ridge (Verdon and Franks, 2006; Verdon-Kidd and Kiem, 2009; Timbal et al., 2010; Gallant et al., 2013; Almedeij, 2015). Although climate indices, including SOI, PDO, IOD, EMI and SSTs, were utilized in different combinations to model the SPI time-series, the greater importance of SST and the respective month in the model's training period as a predictor was evident. Lyon *et al*. (2012) showed a significant improvement in SPI prediction using seasonality in precipitation as an important characteristic of the local climate. In general, seasonality in the precipitation variance was seen to appreciably enhance the predictive skills derived from the drought indicator with substantial variation, depending on the location and season considered. In our study, the use of seasonality was very important for accurately modelling SPI at all study sites, leading to a marked improvement in model performance (Tables 5, 6 and 7). Therefore, our results reinforce the importance of periodicity as an important determinant of drought modelling accuracy.

Comparison of model accuracies using the relative percentage error (*MAPE*) for MARS, LSSVM and M5Tree showed that MARS was more accurate than LSSVM and M5Tree for Bathurst Agricultural Station, and Peak Hill and Yamba stations, whereas for Collarenebri and Barraba, M5Tree was more accurate than other models (Table 7). In fact, the testing of models with and without periodicity found significant differences in the predictive skills, where *MAPE* was recorded to be lower by about 35.93% (Bathurst Agricultural Station), 23.56% (Collarenebri), 64.24% (Peak Hill), 26.21% (Barraba) and 75.45% (Yamba). This demonstrated that the relative contribution of data patterns and attributes in respect to periodicity of SPI-based models varied greatly by the geographic location (Fig. 2). In particular, stations Yamba and Peak Hill were found to be highly responsive to the periodicity as an input variable with a marked improvement in model accuracy, and, therefore, revealed a better potential with greater accuracy

of models at these stations compared to Bathurst, Collarenebri and Barraba. Although the exact cause of this is not known, it is possible that the changes in rainfall and other drought indicators (e.g. SOI) were more closely linked to the cyclic behavior of ocean and atmospheric phases. Earlier studies that developed data-driven models based on a combination of climate indices, SSTs and rainfall found similar variability of the model accuracy over large, sparsely distributed areas (Abbot and Marohasy, 2012, 2014; Deo and Şahin, 2015b, a; Deo et al., 2016b). Therefore, the importance of identifying the most appropriate predictor variable for monthly SPI forecasting remains a paramount task for accurate modelling of drought behavior.

The distinct geographic behaviour of the drought model accuracy was clearly consistent with an earlier study that developed an ANN model for the prediction of the Standardized Precipitation and Evapotranspiration Index (Deo and Şahin, 2015a) and the Effective Drought Index (Deo and Şahin, 2015b). The former study, which also employed rainfall, climate indices and SST data, reported better estimation accuracy for Yamba than for Bathurst Agricultural Station. Therefore, it is perceived that the accuracy of drought models at different study sites is expected to vary in view of the high variability established in the relationships between climate indices, SSTs and rainfall data over different spatial and temporal domains (Nicholls, 2004; Schepen et al., 2012). The evaluation of models over monthly and seasonal scales showed that LSSVM was generally inferior to MARS and M5Tree (Table 9). While the exact cause of this is not known as the models adopt a black-box approach for extracting predictive features in the training dataset, other studies in evaporation modelling (Kisi, 2015, 2016) also found similar results. Importantly, when drought cases (for months with SPI < 0) were analysed in the test period, the M5Tree model showed dramatically better performance for a majority of the stations in moderate, severe and extreme drought categories.

While our study has demonstrated the potential use of MARS, LSSVM and M5Tree algorithms in SPI modelling, there are limitations of this paper that create opportunities for a follow-up work. One limitation was that selection of the best predictor variables based on an individual model's response for accurately predicting the SPI value (Table 5). However, in addition to the original input signal, the lagged combinations of the inputs that are expected to represent the antecedent behaviour of the respective variable over historical time horizon can be applied. If this is done, the drought model is likely to incorporate the important role of serial correlation (or historical persistence) arising from the respective contributory factor, that may also encapsulate the possible interactions and feedbacks from rainfall, climate indices and SSTS into the soil moisture, groundwater storage, recharge and other hydrological parameters for

developing the drought model. Owing to the elusive definition of drought and its insidious and complex nature where the effect of a predictor is not known *a priori*, the information deduced from serial correlation of the inputs could incorporate the inherent persistence characteristics, and therefore, help extract predictive information to improve the future drought warning (Lyon et al., 2012). In fact, the cumulative, time-integrated nature of drought events (resulting in persistence from one month to the next) was shown to be an important time-lagged driver with characteristics valuable for drought monitoring and warning (Redmond, 2002; Nicholls, 2005; Sen and Boken, 2005).

In this study, we did not adopt a pre-processing technique for input data for developing the respective drought models. One criticism of data-driven models without a pre-processing technique is their inability to account for the physics of the hydrological processes (Aksoy et al., 2007) that are necessary for accurate prediction of drought behavior. As the predictors of drought also exhibit nonlinear and non-stationary phenomenon, the presence of non-stationarity features (e.g. trends, seasonal variations, periodicity and jumps in input data) can influence the model accuracy (Tiwari and Chatterjee, 2010; Tiwari and Adamowski, 2013). Also, the relationships between inputs (e.g. rainfall, SOI) and the objective variable is generally non-linear (Montanari et al., 1996), so the non-stationarities caused by trends and seasonal variation can produce a negative impact on model performance (Adamowski et al., 2012; Deo et al., 2016b; Deo et al., 2016c). However, if a pre-processing technique (e.g. wavelet transformation) is adopted, it can extract the time-frequency information and capture the data attributes and patterns to reflect the stochasticity of input variables (Daubechies, 1990). Wavelet transformation is used as an ancillary tool for analyzing stochastic variations, periodicity and trends (Kim and Valdés, 2003; Wang and Ding, 2003; Adamowski and Sun, 2010; Kisi, 2010; Kisi and Cimen, 2011; Nalley et al., 2012; Deo et al., 2016b; Deo et al., 2016c) but is yet to be tested for drought forecasting using MARS, LSSVM and M5Tree. In a follow-up study, wavelet transformation or an alternative data pre-processing tool can be applied to enhance the performance of the prescribed drought models. Additionally, the importance of, and the relationship between, oceanic-atmospheric drivers (e.g. SST) and the respective drought index (e.g. SPI) could potentially be identified by incorporating nonlinear input variable selection (May et al., 2008; Salcedo-Sanz et al., 2014; Seo et al., 2014; Quilty et al., 2016), providing an alternative pathway for deducing the most relevant input variables for improved performance of SPI models.

6.0 Conclusion

Drought forecasting that can yield a numerical evaluation of drought using standardized rainfall deficits and surpluses, and therefore, is an essential task for implementing drought mitigation strategies. A drought poses multi-dimensional, pernicious and detrimental impacts, so the forecasting of SPI which is a universally-acceptable statistical metric for drought assessment, can assist in decision-making for agriculture, water management and water demand, pricing and policy for managing the risks associated with the evolution of a current drought in the future. In this study, the capability of MARS, LSSVM and M5Tree models for SPI modelling was validated for a set of five study sites in drought-prone, eastern Australia. The models were developed using predictor variables defined by rainfall, climate indices and SSTs over the period 1915–2012, that were partitioned in the 50% (training) and 25-25% (cross validation and testing) subsets. In order to test the relative importance of predictor variables for SPI-forecasting, the number of inputs in the MARS model was incremented one by one and the model's performance was assessed using *RMSE*/*MAE* and r^2 between forecasted and observed SPI in training, validation and testing sets. Results revealed that MARS required rainfall and periodicity as mandatory input for all stations, however, the order of importance of SST and climate indices was unique among the different stations. This confirmed the superior role of a given predictor variable over others, in respect of SPI modelling at the respective study site. Comparison of the data-driven models revealed that MARS and M5Tree can be successfully adopted for SPI forecasting, although there was a significant geographic variation in the performance of models. While MARS exhibited the highest accuracy for Bathurst and Peak Hill stations with *MAPE* = 29.05% and 25.79%, respectively, the M5Tree accuracy exceeded MARS and LSSVM for Collarenebri, Barraba and Yamba with *MAPE* = 29.098%, 37.94% and 20.89%, respectively. Importantly, the assessment of drought cases in the test data showed that M5Tree was highly qualified for modelling drought part of the SPI data. In the case of forecasting moderate drought in the range $-1.5 \leq SPI\ -0.5$, the mean absolute percentage error for M5Tree was between 5.9–13.6% for the four study sites (Collarenebri, Peak Hill, Barraba and Yamba). For severe drought, the accuracy of MARS exceeded LSSVM and M5Tree for Collarenebri, Peak Hill and Barraba, whereas for severe drought cases, MARS was more accurate than the other two models for Bathurst, Collarenebri and Barraba and Yamba stations. It is noteworthy that LSSVM was generally inferior for SPI forecasting when drought segment of SPI was considered although the model's hyperparameters (kernel width and regularization constant) were optimized using grid-search procedures to enhance the forecasting accuracy. No doubt, our study showed the complexity of drought modeling in eastern Australia, where no single forecasting model was seen to be universally better than the other for all study sites considered. Therefore, it is

advocated that the selection of drought models based on a given data-driven techniques is not achievable without challenges, thus, drought modelling may be tackled appropriately by enhancing the understanding and complexity of model inputs (predictor variables) in relation to the drought behavior and how these patterns and attributes are extracted to develop the actual drought forecasts. Finally, a drought model accuracy is expected to be only dependent on the considered model's mathematical and computational frameworks but also on the interactions of the predictive features within the input variables utilized and the non-linear associations with the respective response variable (drought index).

Acknowledgment

The precipitation data were from Australian Bureau of Meteorology and climate indices and SST from the Joint Institute of Study of Atmosphere and Ocean and Japanese Agency for Marine-Earth Science and Technology. USQ Academic Division funded first author (Dr RC Deo) through "Research Activation Incentive Scheme (RAIS, July–September 2015)" to collaborate with Professor Ozgur Kisi (Canik Basari University, Turkey) and Distinguished Professor Vijay P. Singh, Texas A&M University (USA). Dr RC Deo held Endeavour Executive Fellowship (4293–2015) funded by the Australian Government. We also thank the reviewer and Editor-in-Chief for their insightful comments on this paper.

Figure Captions

Fig. 1. Structures of MARS, M5Tree and LSSVM models.

Fig. 2 Monthly standarized precipitation index with drought characteristics and rainfall data for millennium drought (January 2002–April 2003) for Bathurst Agricultural Station.

Fig. 3 Location of study sites in eastern New South Wales (NSW).

Fig. 4 The variation of test root mean square error (RMSE) versus regularisation constant (C) and kernel width (σ) for LSSVR model for Bathurst Agricultural Station.

Fig. 5 Scatterplot of forecasted (SPI_F) and observed (SPI_O) standardized precipitation index (*SPI*) using the MARS model with and without periodicity (i.e. month) as an input parameter with a linear regression equation.

Fig. 6 Forecasting error, $E = SPI_F - SPI_O$ for MARS, LSSVM and M5Tree (with periodicity as an input variable) in the last 5 years of testing period.

Fig. 7 Frequency distribution of forecasting error encountered by optimum MARS, LSSVM and M5Tree models.

Table Captions

Table 1: Descriptive statistics of the study sites.

Table 2: Input variables used for monthly *SPI* forecasting.

Table 3: The partitioning of input data into training, validation and testing sets.

Table 4: Cross correlation of inputs (with *SPI*). r_{cross} in boldface are statistically significant with 95% confidence.

Table 5: Influence of input combinations for forecasting of *SPI* using a MARS model measured by root mean square error (RMSE), mean absolute error (MAE) and coefficient of determination (R^2). Note: optimum model for each site is **boldfaced** (blue).

Table 6: Comparison of MARS, M5 Tree and LSSVM models with optimum inputs with and without periodicity.

Table 7: Comparison of optimum MARS, LSSVM and M5Tree according to Willmott's index (*WI*) and mean absolute percentage error (MAPE, %) with and without periodicity.

Table 8: Forecasting skill of optimum MARS, M5Tree and LSSVM in terms of mean absolute percentage error, MAPE (%) for different categories of drought events within the test period.

Table 9: Analysis of mean absolute percentage error, MAPE (%), over seasonal scales.

Table A1 The regression tree for the optimal MARS models in modeling SPI-Bathurst

Table A2 The regression tree for the optimal M5Tree models in modeling SPI-Bathurst.

References

Abbot, J., Marohasy, J.2012.Application of artificial neural networks to rainfall forecasting in Queensland, Australia *Adv. Atmos. Sci.* **29**, pp. 717-730.

Abbot, J., Marohasy, J.2014.Input selection and optimisation for monthly rainfall forecasting in Queensland, Australia, using artificial neural networks *Atmos. Res.* **138**, pp. 166-178.

Abraham, A., Steinberg, D. 2001 Is neural network a reliable forecaster on earth? a MARS query! , *Bio-Inspired Applications of Connectionism*, Springer, pp. 679-686.

Adamowski, J., Fung Chan, H., Prasher, S.O., Ozga‐Zielinski, B., Sliusarieva, A.2012.Comparison of multiple linear and nonlinear regression, autoregressive integrated moving average, artificial neural network, and wavelet artificial neural network methods for urban water demand forecasting in Montreal, Canada *Water Resour. Res.* **48**.

Adamowski, J., Karapataki, C.2010.Comparison of multivariate regression and artificial neural networks for peak urban water-demand forecasting: evaluation of different ANN learning algorithms *Journal of Hydrologic Engineering* **15**, pp. 729-743.

Adamowski, J., Sun, K.2010.Development of a coupled wavelet transform and neural network method for flow forecasting of non-perennial rivers in semi-arid watersheds *J. Hydrol.* **390**, pp. 85-91.

Aksoy, H., Guven, A., Aytek, A., Yuce, M.I., Unal, N.E.2007.Discussion of "Generalized regression neural networks for evapotranspiration modelling" *Hydrological Sciences Journal* **52**, pp. 825-831.

Alexander, L. *et al.*2006.Global observed changes in daily climate extremes of temperature and precipitation *Journal of Geophysical Research: Atmospheres (1984–2012)* **111**.

Alexandersson, H.1986.A homogeneity test applied to precipitation data *Journal of climatology* **6**, pp. 661-675.

Almedeij, J.2015.Long-term periodic drought modeling *Stochastic Environmental Research and Risk Assessment*, pp. 1-10.

Ashok, K., Behera, S.K., Rao, S.A., Weng, H., Yamagata, T.2007.El Niño Modoki and its possible teleconnection *Journal of Geophysical Research: Oceans (1978–2012)* **112**.

Bates, B., Kundzewicz, Z.W., Wu, S., Palutikof, J. 2008 *Climate change and water: Technical paper vi*. Intergovernmental Panel on Climate Change (IPCC).

Belayneh, A., Adamowski, J.2012.Standard precipitation index drought forecasting using neural networks, wavelet neural networks, and support vector regression *Applied Computational Intelligence and Soft Computing* **2012**, p. 6.

Bhattacharya, B., Solomatine, D.P.2005.Neural networks and M5 model trees in modelling water level–discharge relationship *Neurocomputing* **63**, pp. 381-396.

Bishop, C.M. 1995 *Neural networks for pattern recognition*. Oxford university press.

BOM High-quality Australian Daily Rainfall Dataset. National Climate Centre, Bureau of Meteorology, Melbourne, Victoria (2008).

Brown, S.C., Versace, V.L., Lester, R.E., Walter, M.T.2015.Assessing the impact of drought and forestry on streamflows in south-eastern Australia using a physically based hydrological model *Environmental Earth Sciences* **74**, pp. 6047-6063.

Butte, N.F. *et al.*2010.Validation of cross-sectional time series and multivariate adaptive regression splines models for the prediction of energy expenditure in children and adolescents using doubly labeled water *The Journal of nutrition* **140**, pp. 1516-1523.

Cai, W., Cowan, T.2008.Evidence of impacts from rising temperature on inflows to the Murray‐Darling Basin *Geophysical research letters* **35**.

Cai, W., Cowan, T.2009.La Niña Modoki impacts Australia autumn rainfall variability *Geophysical Research Letters* **36**.

Cancelliere, A., Bonaccorso, B., Mauro, G.2006.A non-parametric approach for drought forecasting through the standardized precipitation index *Metodi statisticie matematici per l Analisi delle serie idrologiche* **1**, pp. 1-8.

Cancelliere, A., Di Mauro, G., Bonaccorso, B., Rossi, G.2007.Drought forecasting using the standardized precipitation index *Water. Resour. Manag.* **21**, pp. 801-819.

Cheng, M.-Y., Cao, M.-T.2014.Accurately predicting building energy performance using evolutionary multivariate adaptive regression splines *Applied Soft Computing* **22**, pp. 178-188.

Cherkassky, V., Mulier, F.M. 2007 *Learning from data: concepts, theory, and methods*. John Wiley & Sons.

Choubin, B., Malekian, A., Gloshan, M.2016.Application of several data-driven techniques to predict a standardized precipitation index *Atmósfera* **29**, pp. 121-128.

Craven, P., Wahba, G.1978.Smoothing noisy data with spline functions *Numerische Mathematik* **31**, pp. 377-403.

Crimp, S. *et al.*2015.Bayesian space–time model to analyse frost risk for agriculture in Southeast Australia *Int. J. Climatol.* **35**, pp. 2092-2108.

Daubechies, I.1990.The wavelet transform, time-frequency localization and signal analysis *Information Theory, IEEE Transactions on* **36**, pp. 961-1005.

Dawson, C.W., Abrahart, R.J., See, L.M.2007.HydroTest: a web-based toolbox of evaluation metrics for the standardised assessment of hydrological forecasts *Environmental Modelling & Software* **22**, pp. 1034-1052.

Deo, R.C., Byun, H.-R., Adamowski, J.F., Begum, K.2016a.Application of effective drought index for quantification of meteorological drought events: a case study in Australia *Theoretical and Applied Climatology*, pp. 1-21.

Deo, R.C., Şahin, M.2015a.Application of the Artificial Neural Network model for prediction of monthly Standardized Precipitation and Evapotranspiration Index using hydrometeorological parameters and climate indices in eastern Australia *Atmos. Res.* **161-162**, pp. 65-81.

Deo, R.C., Şahin, M.2015b.Application of the extreme learning machine algorithm for the prediction of monthly Effective Drought Index in eastern Australia *Atmos. Res.* **153**, pp. 512-525.

Deo, R.C., Şahin, M.2016.An extreme learning machine model for the simulation of monthly mean streamflow water level in eastern Queensland *Environmental Monitoring and Assessment* **DOI (10.1007/s10661-016-5094-9)**.

Deo, R.C., Samui, P., Kim, D.2015.Estimation of monthly evaporative loss using relevance vector machine, extreme learning machine and multivariate adaptive regression spline models *Stochastic Environmental Research and Risk Assessment*, pp. 1-16.

Deo, R.C. *et al.*2009.Impact of historical land cover change on daily indices of climate extremes including droughts in eastern Australia *Geophysical Research Letters* **36**.

Deo, R.C., Tiwari, M.K., Adamowski, J., Quilty, J.2016b.Forecasting Effective Drought Index Using a Wavelet Extreme Learning Machine (W-ELM) Model *Stochastic Environmental Research and Risk Assessment* **in press**, pp. DOI: 10.1007/s00477-00016-01265-z.

Deo, R.C., Wen, X., Feng, Q.2016c.A wavelet-coupled support vector machine model for forecasting global incident solar radiation using limited meteorological dataset *Applied Energy* **168**, pp. 568–593.

Dijk, A.I. *et al.*2013.The Millennium Drought in southeast Australia (2001–2009): Natural and human causes and implications for water resources, ecosystems, economy, and society *Water Resour. Res.* **49**, pp. 1040-1057.

Friedman, J.H.1991.Multivariate adaptive regression splines *The annals of statistics*, pp. 1-67.

Gallant, A.J., Reeder, M.J., Risbey, J.S., Hennessy, K.J.2013.The characteristics of seasonal‐scale droughts in Australia, 1911–2009 *Int. J. Climatol.* **33**, pp. 1658-1672.

Goyal, M.K., Bharti, B., Quilty, J., Adamowski, J., Pandey, A.2014.Modeling of daily pan evaporation in sub tropical climates using ANN, LS-SVR, Fuzzy Logic, and ANFIS *Expert Systems with Applications* **41**, pp. 5267-5276.

Guttman, N.B. Accepting the standardized precipitation index: A calculation algorithm1. Wiley Online Library (1999).

Hayes, M.J., Svoboda, M., Wall, N., Widhalm, M.2011.The Lincoln declaration on drought indices: universal meteorological drought index recommended *Bulletin of the American Meteorological Society* **92**, pp. 485-488.

Hayes, M.J., Svoboda, M.D., Wilhite, D.A., Vanyarkho, O.V.1999.Monitoring the 1996 drought using the standardized precipitation index *Bulletin of the American Meteorological Society* **80**, pp. 429-438.

Haylock, M., Nicholls, N.2000.Trends in extreme rainfall indices for an updated high quality data set for Australia, 1910-1998 *Int. J. Climatol.* **20**, pp. 1533-1541.

Helman, P. Droughts in the Murrary-Darling Basin since European settlement. Griffith Centre for Coastal Management Research Report No 100, Licensed from the Murray-Darling Basin Authority under a Creative Commons Attribution 3.0 Australia Licence (2009).

Hsu, C.-W., Chang, C.-C., Lin, C.-J. A practical guide to support vector classification. (2003).

Hsu, H.-H., Hung, C.-H., Lo, A.-K., Wu, C.-C., Hung, C.-W.2008.Influence of tropical cyclones on the estimation of climate variability in the tropical western North Pacific *J. Climatol.* **21**, pp. 2960-2975.

IPCC 2007 *Summary for Policymakers. In: Climate Change 2007: The Physical Science Basis. Contribution of Working Group I to the Fourth Assessment Report of the Intergovernmental Panel on Climate Change* Cambridge University Press, United Kingdom and New York, NY, USA 1-18 pp.

IPCC 2012 Summary for Policymakers: A Special Report of Working Groups I and II of the Intergovernmental Panel on Climate Change. in: Field, C.B. *et al.* (Eds.), *In: Managing the Risks of Extreme Events and Disasters to Advance Climate Change Adaptation* Cambridge University Press, Cambridge, UK.

Jalalkamali, A., Moradi, M., Moradi, N.2015.Application of several artificial intelligence models and ARIMAX model for forecasting drought using the Standardized Precipitation Index *International Journal of Environmental Science and Technology* **12**, pp. 1201-1210.

Joaquín Andreu *et al.* 2015 Drought Indicators: Monitoring, Forecasting and Early Warning at the Case Study Scale. *DROUGHT-R&SPI (Fostering European Drought Research and Science-Policy Interfacing) , Collaborative Project funded by the European Commission under the FP7 Cooperation Work Programme: Theme 6: Environment (Grant agreement no: 282769).*

Jones, P. *et al.*1996.Summer moisture availability over Europe in the Hadley Centre general circulation model based on the Palmer Drought Severity Index *Int. J. Climatol.* **16**, pp. 155-172.

Kane, R.1997.Prediction of Droughts in North‐East Brazil: Role of ENSO and Use of Periodicities *Int. J. Climatol.* **17**, pp. 655-665.

Kane, R.P., Trivedi, N.B.1986.Are droughts predictable? *Climatic Change* **8**, pp. 209-223.

Keyantash, J., Dracup, J.A.2002.The quantification of drought: an evaluation of drought indices *Bulletin of the American Meteorological Society* **83**, pp. 1167-1180.

Kim, T.-W., Valdés, J.B.2003.Nonlinear model for drought forecasting based on a conjunction of wavelet transforms and neural networks *Journal of Hydrologic Engineering* **8**, pp. 319-328.

Kisi, O.2010.Wavelet regression model for short-term streamflow forecasting *J. Hydrol.* **389**, pp. 344-353.

Kisi, O.2015.Pan evaporation modeling using least square support vector machine, multivariate adaptive regression splines and M5 model tree *J. Hydrol.* **528**, pp. 312-320.

Kisi, O.2016.Modeling reference evapotranspiration using three different heuristic regression approaches *Agricultural Water Management* **169**, pp. 162-172.

Kisi, O., Cimen, M.2011.A wavelet-support vector machine conjunction model for monthly streamflow forecasting *J. Hydrol.* **399**, pp. 132-140.

Koehn, J.2015.Managing people, water, food and fish in the Murray‐Darling Basin, south‐eastern Australia *Fisheries Management and Ecology* **22**, pp. 25-32.

Krause, P., Boyle, D., Bäse, F.2005.Comparison of different efficiency criteria for hydrological model assessment *Advances in Geosciences* **5**, pp. 89-97.

Lavery, B., Joung, G., Nicholls, N.1997.An extended high-quality historical rainfall dataset for Australia *Australian Meteorological Magazine* **46**, pp. 27-38.

Legates, D.R., McCabe, G.J.1999.Evaluating the use of "goodness‐of‐fit" measures in hydrologic and hydroclimatic model validation *Water Resour. Res.* **35**, pp. 233-241.

Lin, H.-T., Lin, C.-J.2003.A study on sigmoid kernels for SVM and the training of non-PSD kernels by SMO-type methods *submitted to Neural Computation*, pp. 1-32.

Lyon, B. *et al.*2012.Baseline probabilities for the seasonal prediction of meteorological drought *Journal of Applied Meteorology and Climatology* **51**, pp. 1222-1237.

Mantua, N.J., Hare, S.R., Zhang, Y., Wallace, J.M., Francis, R.C.1997.A Pacific interdecadal climate oscillation with impacts on salmon production *Bulletin of the american Meteorological Society* **78**, pp. 1069-1079.

Marj, A.F., Meijerink, A.M.2011.Agricultural drought forecasting using satellite images, climate indices and artificial neural network *International journal of remote sensing* **32**, pp. 9707-9719.

May, R.J., Maier, H.R., Dandy, G.C., Fernando, T.G.2008.Non-linear variable selection for artificial neural networks using partial mutual information *Environmental Modelling & Software* **23**, pp. 1312-1326.

McAlpine, C. *et al.*2007.Modeling the impact of historical land cover change on Australia's regional climate *Geophysical Research Letters* **34**.

McAlpine, C. *et al.*2009.A continent under stress: interactions, feedbacks and risks associated with impact of modified land cover on Australia's climate *Global Change Biology* **15**, pp. 2206-2223.

McGowan, H.A., Marx, S.K., Denholm, J., Soderholm, J., Kamber, B.S.2009.Reconstructing annual inflows to the headwater catchments of the Murray River, Australia, using the Pacific Decadal Oscillation *Geophysical Research Letters* **36**.

McKee, T.B., Doesken, N.J., Kleist, J. The relationship of drought frequency and duration to time scales. *Proceedings of the 8th Conference on Applied Climatology*, American Meteorological Society Boston, MA (1993), pp. 179-183.

McKeon, G., Hall, W., Henry, B., Stone, G., Watson, I.2004.Pasture degradation and recovery in Australia's rangelands: learning from history.

Mishra, A.K., Desai, V.2005.Drought forecasting using stochastic models *Stochastic Environmental Research and Risk Assessment* **19**, pp. 326-339.

Mishra, A.K., Singh, V.P.2010.A review of drought concepts *J. Hydrol.* **391**, pp. 202-216.

Mishra, A.K., Singh, V.P.2011.Drought modeling–A review *J. Hydrol.* **403**, pp. 157-175.

Mitchell, T.M.1997.Machine learning *Computer Science Series (McGraw-Hill, Burr Ridge, 1997) MATH*.

Montanari, A., Rosso, R., Taqqu, M.S.1996.Some long‐run properties of rainfall records in Italy *Journal of Geophysical Research: Atmospheres (1984‐2012)* **101**, pp. 29431-29438.

Moreira, E., Martins, D., Pereira, L.2015.Assessing drought cycles in SPI time series using a Fourier analysis *Natural Hazards and Earth System Sciences* **15**, pp. 571-585.

Mpelasoka, F., Hennessy, K., Jones, R., Bates, B.2008.Comparison of suitable drought indices for climate change impacts assessment over Australia towards resource management *Int. J. Climatol.* **28**, pp. 1283-1292.

Müller, K.-R. *et al.* 1997 Predicting time series with support vector machines. *Artificial Neural Networks—ICANN'97*, Springer Berlin Heidelberg, Switzerland, pp. 999-1004.

Nalley, D., Adamowski, J., Khalil, B.2012.Using discrete wavelet transforms to analyze trends in streamflow and precipitation in Quebec and Ontario (1954–2008) *J. Hydrol.* **475**, pp. 204-228.

Nicholls, N.2004.The changing nature of Australian droughts *Climatic change* **63**, pp. 323-336.

Nicholls, N., M. J. Coughlan, and K. Monnik, 2005 2005 The Challenge of Climate Prediction in Mitigating Drought Impacts. in: Wilhite, D.A. (Ed.), *Drought and Water Crises: Drought andWater Crises, Science Technology and Management Issues,*, Taylor and Francis: , 33–51., p. 33.

Okkan, U., Serbes, Z.A.2012.Rainfall–runoff modeling using least squares support vector machines *Environmetrics* **23**, pp. 549-564.

Power, S. *et al.*1999.Decadal climate variability in Australia during the twentieth century *Int. J. Climatol.* **19**, pp. 169-184.

Quilty, J., Adamowski, J., Khalil, B., Rathinasamy, M.2016.Bootstrap rank ‐ ordered conditional mutual information (broCMI)−A nonlinear input variable selection method for water resources modeling *Water Resour. Res.*

Quinlan, J.R. Learning with continuous classes. *5th Australian joint conference on artificial intelligence*, Singapore (1992), pp. 343-348.

Qureshi, M., Ahmad, M., Whitten, S., Reeson, A., Kirby, M.2016.Impact of Climate Variability Including Drought on the Residual Value of Irrigation Water Across the Murray–Darling Basin, Australia *Water Economics and Policy*, p. 1550020.

Rahimikhoob, A., Asadi, M., Mashal, M.2013.A comparison between conventional and M5 model tree methods for converting pan evaporation to reference evapotranspiration for semi-arid region *Water. Resour. Manag.* **27**, pp. 4815-4826.

Rahmat, S.N., Jayasuriya, N., Bhuiyan, M.A.2016.Short-term droughts forecast using Markov chain model in Victoria, Australia *Theoretical and Applied Climatology*, pp. 1-13.

Redmond, K.2002.The depiction of drought—A commentary *Bulletin of American Meteorological Society* **83**, pp. 1143-1147.

Riebsame, W.E., Changnon Jr, S.A., Karl, T.R. 1991 *Drought and natural resources management in the United States. Impacts and implications of the 1987-89 drought*. Westview Press Inc.

Salcedo-Sanz, S., Pastor-Sánchez, A., Prieto, L., Blanco-Aguilera, A., García-Herrera, R.2014.Feature selection in wind speed prediction systems based on a hybrid coral reefs optimization–Extreme learning machine approach *Energy Conversion and Management* **87**, pp. 10-18.

Samui, P.2012.Slope stability analysis using multivariate adaptive regression spline *Metaheuristics in Water, Geotechnical and Transport Engineering*, p. 327.

Santos, C.A.G., Morais, B.S., Silva, G.B.2009.Drought forecast using an artificial neural network for three hydrological zones in San Francisco River basin, Brazil *IAHS publication* **333**, p. 302.

Schepen, A., Wang, Q., Robertson, D.2012.Evidence for using lagged climate indices to forecast Australian seasonal rainfall *J. Climatol.* **25**, pp. 1230-1246.

Şen, Z. 2015 *Applied Drought Modeling*. Elsevier (205), 484 pp.

Sen, Z., Boken, V.K. 2005 *Techniques to predict agricultural droughts*. Oxford University Press.

Seo, J.-H., Lee, Y.H., Kim, Y.-H.2014.Feature selection for very short-term heavy rainfall prediction using evolutionary computation *Advances in Meteorology* **2014**.

Sephton, P.2001.Forecasting recessions: Can we do better on mars *Federal Reserve Bank of St. Louis Review* **83**.

Sharda, V., Prasher, S., Patel, R., Ojasvi, P., Prakash, C.2008.Performance of Multivariate Adaptive Regression Splines (MARS) in predicting runoff in mid-Himalayan micro-watersheds with limited data/Performances de régressions par splines multiples et adaptives (MARS) pour la prévision d'écoulement au sein de micro-bassins versants Himalayens d'altitudes intermédiaires avec peu de données *Hydrological sciences journal* **53**, pp. 1165-1175.

Sheffield, J., Wood, E.F.2008.Projected changes in drought occurrence under future global warming from multi-model, multi-scenario, IPCC AR4 simulations *Clim. Dyn.* **31**, pp. 79-105.

Shirmohammadi, B., Moradi, H., Moosavi, V., Semiromi, M.T., Zeinali, A.2013.Forecasting of meteorological drought using Wavelet-ANFIS hybrid model for different time steps (case study: southeastern part of east Azerbaijan province, Iran) *Natural hazards* **69**, pp. 389-402.

Stahl, K., van Lanen, H. Guidelines for monitoring and early warning of drought in Europe. DROUGHT-R&SPI (2014).

Suppiah, R., Hennessy, K.J.1998.Trends in total rainfall, heavy rain events and number of dry days in Australia, 1910–1990 *Int. J. Climatol.* **18**, pp. 1141-1164.

Suykens, J.A.K., De Brabanter, J., Lukas, L., Vandewalle, J.2002.Weighted least squares support vector machines: robustness and sparse approximation *Neurocomputing* **48**, pp. 85-105.

Suykens, J.A.K., Lukas, L., Van Dooren, P., De Moor, B., Vandewalle, J. Least squares support vector machine classifiers: a large scale algorithm. *European Conference on Circuit Theory and Design, ECCTD*, Citeseer (1999), pp. 839-842.

Suykens, J.A.K., Vandewalle, J.1999.Least squares support vector machine classifiers *Neural processing letters* **9**, pp. 293-300.

Svoboda, M., Hayes, M., Wood, D.2012.Standardized precipitation index user guide *World Meteorological Organization Geneva, Switzerland*.

Timbal, B. *et al.* 2010 *Understanding the anthropogenic nature of the observed rainfall decline across South Eastern Australia*. Centre for Australian Weather and Climate Research.

Timbal, B., Hendon, H.2011.The role of tropical modes of variability in recent rainfall deficits across the Murray‐Darling Basin *Water Resour. Res.* **47**.

Tiwari, M.K., Adamowski, J.2013.Urban water demand forecasting and uncertainty assessment using ensemble wavelet‐bootstrap‐neural network models *Water Resour. Res.* **49**, pp. 6486-6507.

Tiwari, M.K., Chatterjee, C.2010.Development of an accurate and reliable hourly flood forecasting model using wavelet–bootstrap–ANN (WBANN) hybrid approach *J. Hydrol.* **394**, pp. 458-470.

Torok, S., Nicholls, N.1996.A historical annual temperature dataset *Australian Meteorological Magazine* **45**.

Trenberth, K.E.1984.Signal versus noise in the Southern Oscillation *Monthly Weather Review* **112**, pp. 326-332.

Ummenhofer, C.C. *et al.*2009.What causes southeast Australia's worst droughts? *Geophysical Research Letters* **36**.

UN/ISDR Drought Risk Reduction Framework and Practices: Contributing to the Implementation of the Hyogo Framework for Action., *United Nations secretariat of the International Strategy for Disaster Reduction (UN/ISDR)*, Geneva, Switzerland (2007), p. 98+vi pp.

Vapnik, V.N., Vapnik, V. 1998 *Statistical learning theory*. Wiley New York.

Verdon‐Kidd, D.C., Kiem, A.S.2009.Nature and causes of protracted droughts in southeast Australia: Comparison between the Federation, WWII, and Big Dry droughts *Geophysical Research Letters* **36**.

Verdon, D.C., Franks, S.W.2006.Long‐term behaviour of ENSO: Interactions with the PDO over the past 400 years inferred from paleoclimate records *Geophysical Research Letters* **33**.

Vicente-Serrano, S.2016.Foreword: Drought complexity and assessment under climate change conditions *Cuadernos de Investigación Geográfica*.

Wang, W., Ding, J.2003.Wavelet network model and its application to the prediction of hydrology *Nature and Science* **1**, pp. 67-71.

Waseem, M., Ajmal, M., Kim, T.-W.2015.Development of a new composite drought index for multivariate drought assessment *J. Hydrol.* **527**, pp. 30-37.

Weng, H., Ashok, K., Behera, S.K., Rao, S.A., Yamagata, T.2007.Impacts of recent El Niño Modoki on dry/wet conditions in the Pacific rim during boreal summer *Clim. Dyn.* **29**, pp. 113-129.

Weng, H., Behera, S.K., Yamagata, T.2009.Anomalous winter climate conditions in the Pacific rim during recent El Niño Modoki and El Niño events *Clim. Dyn.* **32**, pp. 663-674.

Wilhite, D.A., Hayes, M.J. 1998 Drought planning in the United States: Status and future directions. *The arid frontier*, Springer, pp. 33-54.

Wilhite, D.A., Hayes, M.J., Knutson, C., Smith, K.H. Planning for drought: Moving from crisis to risk management1. Wiley Online Library (2000a).

Wilhite, D.A., Sivakumar, M., Wood, D.A. Early warning systems for drought preparedness and drought management. *Proceedings of an Expert Group Meeting held in Lisbon, Portugal* (2000b), pp. 5-7.

Williams, A. *et al.*2015.Quantifying the response of cotton production in eastern Australia to climate change *Climatic Change* **129**, pp. 183-196.

Willmott, C.J.1981.On the validation of models *Physical geography* **2**, pp. 184-194.

Willmott, C.J. 1984 On the evaluation of model performance in physical geography. *Spatial statistics and models*, Springer, pp. 443-460.

Witten, I.H., Frank, E. 2005 *Data Mining: Practical machine learning tools and techniques*. Morgan Kaufmann.

Wittwer, G., Adams, P.D., Horridge, M., Madden, J.R.2002.Drought, regions and the Australian economy between 2001-02 and 2004-05 *Australian Bulletin of Labour* **28**, p. 231.

Yevjevich, V. 1967 *An objective approach to definitions and investigations of continental hydrologic droughts*. Colorado State University Fort Collins.

Yevjevich, V.1991.Tendencies in hydrology research and its applications for 21st century *Water. Resour. Manag.* **5**, pp. 1-23.

Yuan, W.-P., Zhou, G.-S.2004.Comparison between standardized precipitation index and Z-index in China *Acta Phytoecologica Sinica* **4**.

Zhang, W., Goh, A.2013.Multivariate adaptive regression splines for analysis of geotechnical engineering systems *Computers and Geotechnics* **48**, pp. 82-95.

Zhang, Y., Wallace, J.M., Battisti, D.S.1997.ENSO-like interdecadal variability: 1900-93 *J. Climatol.* **10**, pp. 1004-1020.

Figures

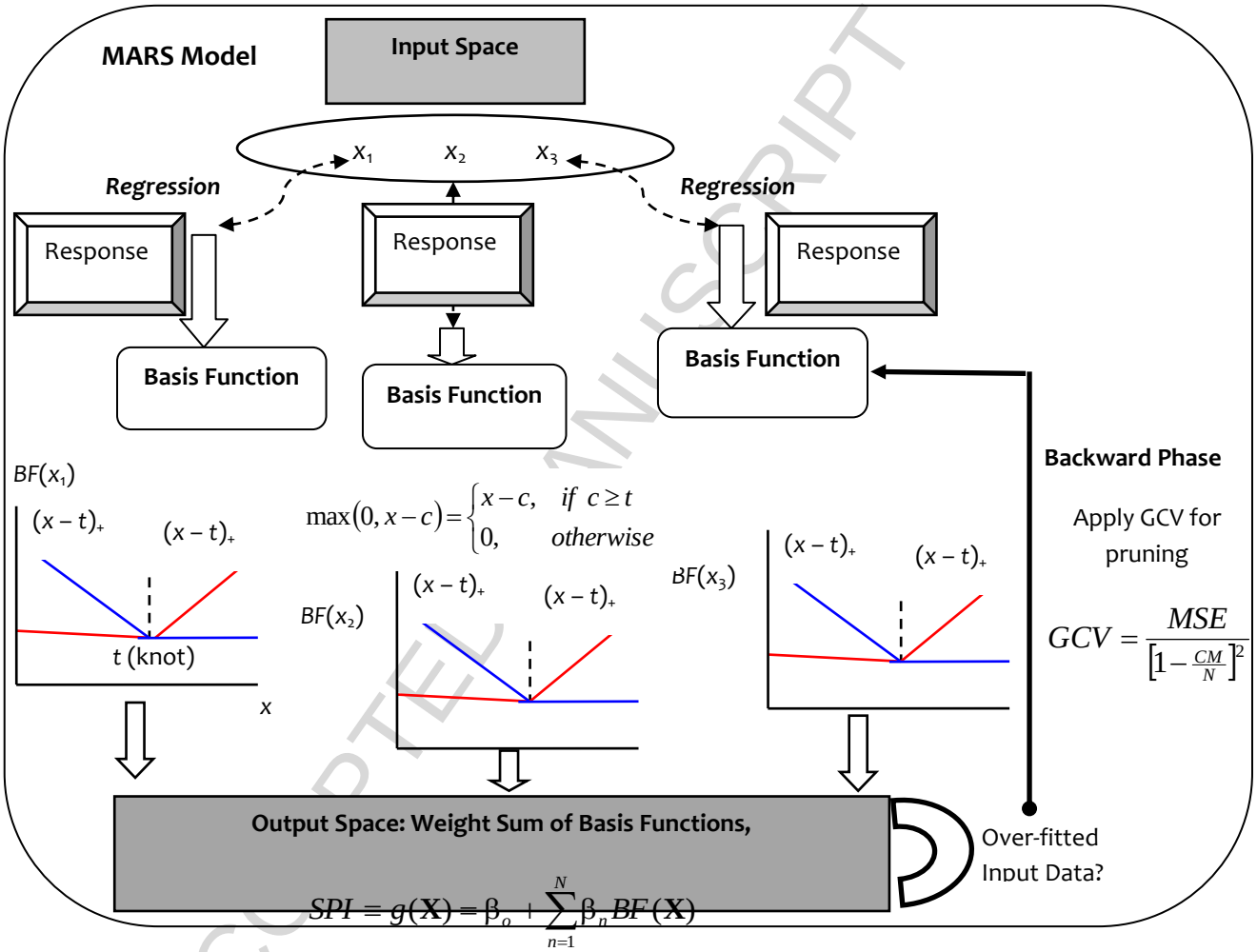

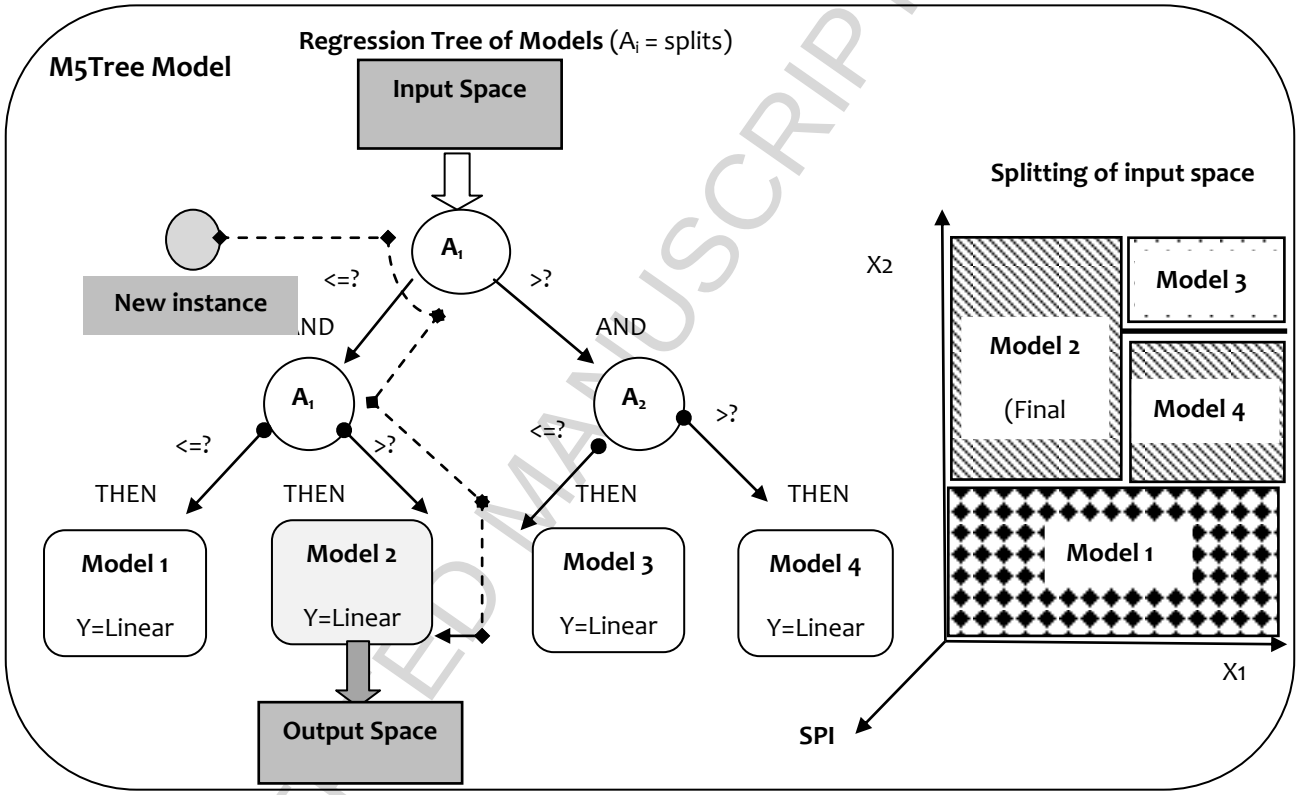

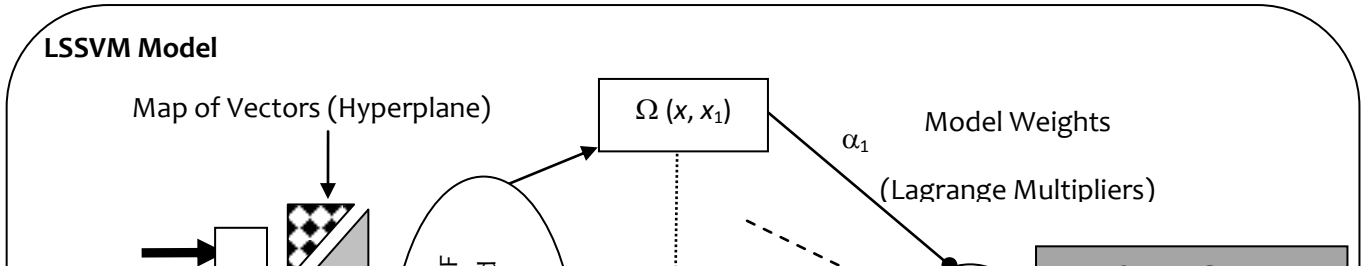

Fig. 1. Structures of MARS, M5Tree and LSSVM models.

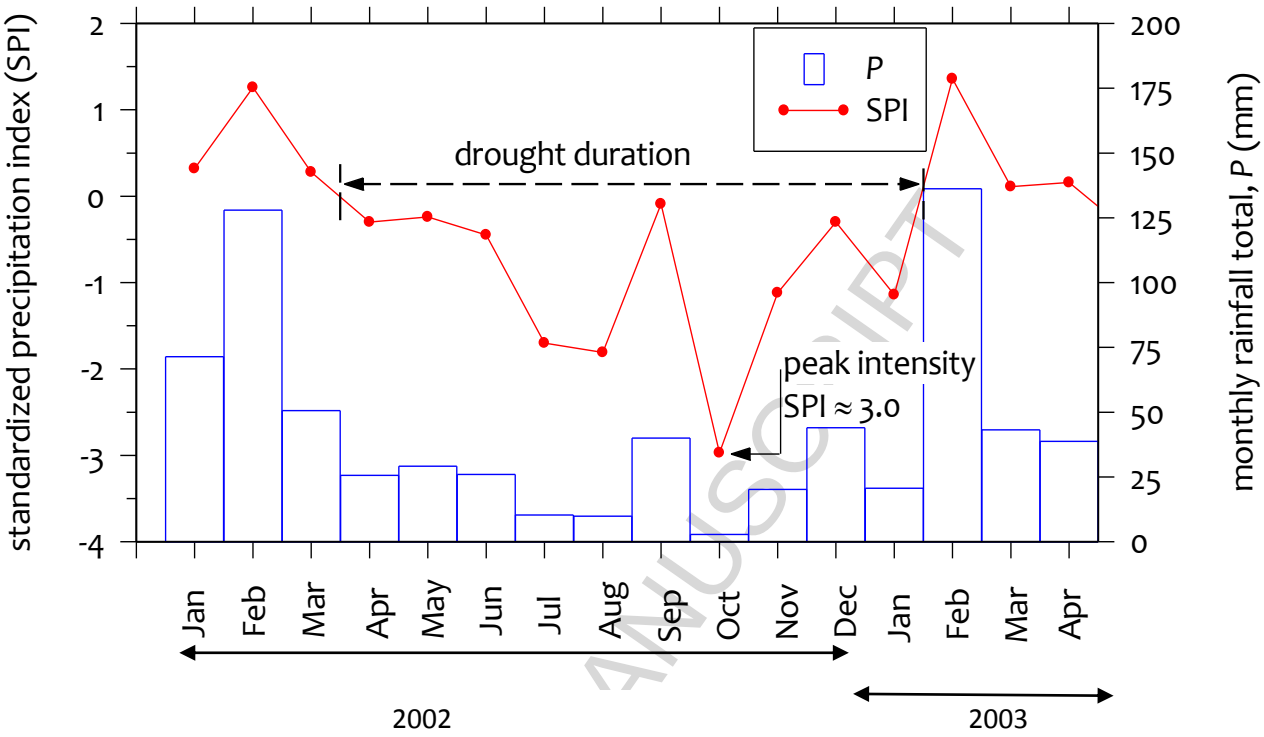

Fig. 2 Monthly standarized precipitation index with drought characteristics and rainfall data for millennium drought (January 2002–April 2003) for Bathurst Agricultural Station.

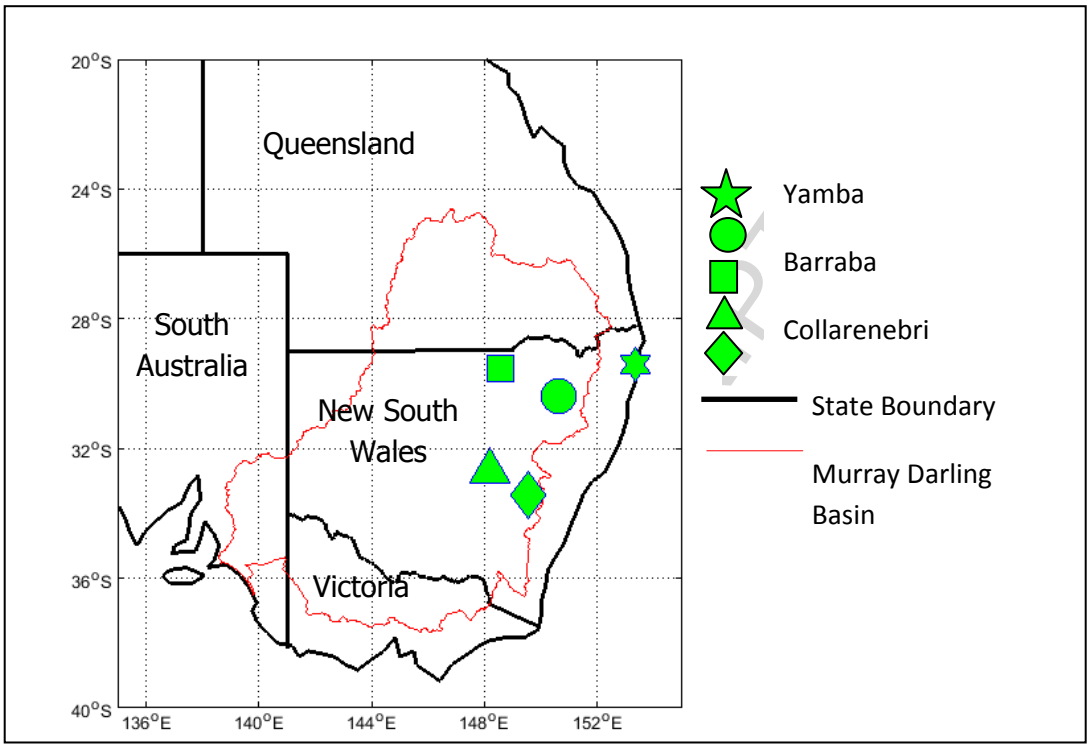

Fig. 3 Location of study sites in eastern New South Wales (NSW).

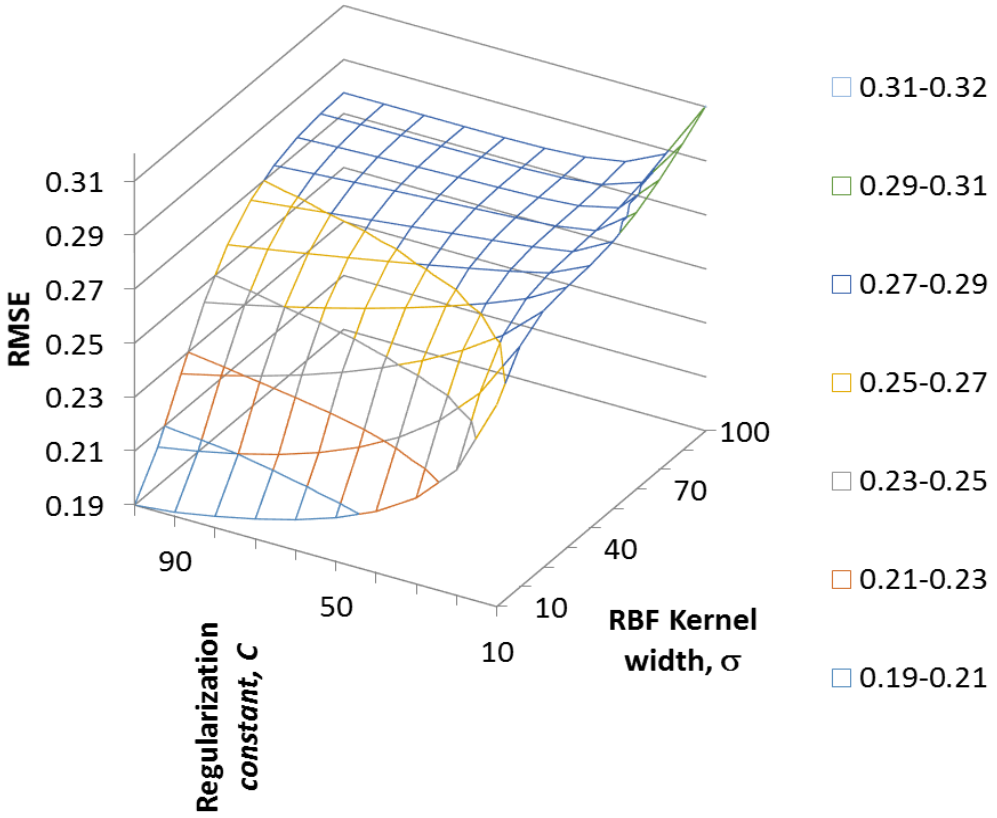

Fig. 4 The variation of test root mean square error (RMSE) versus regularisation constant (C) and kernel width (σ) for LSSVR model for Bathurst Agricultural Station.

MARS Model **MARS (with periodicity)**

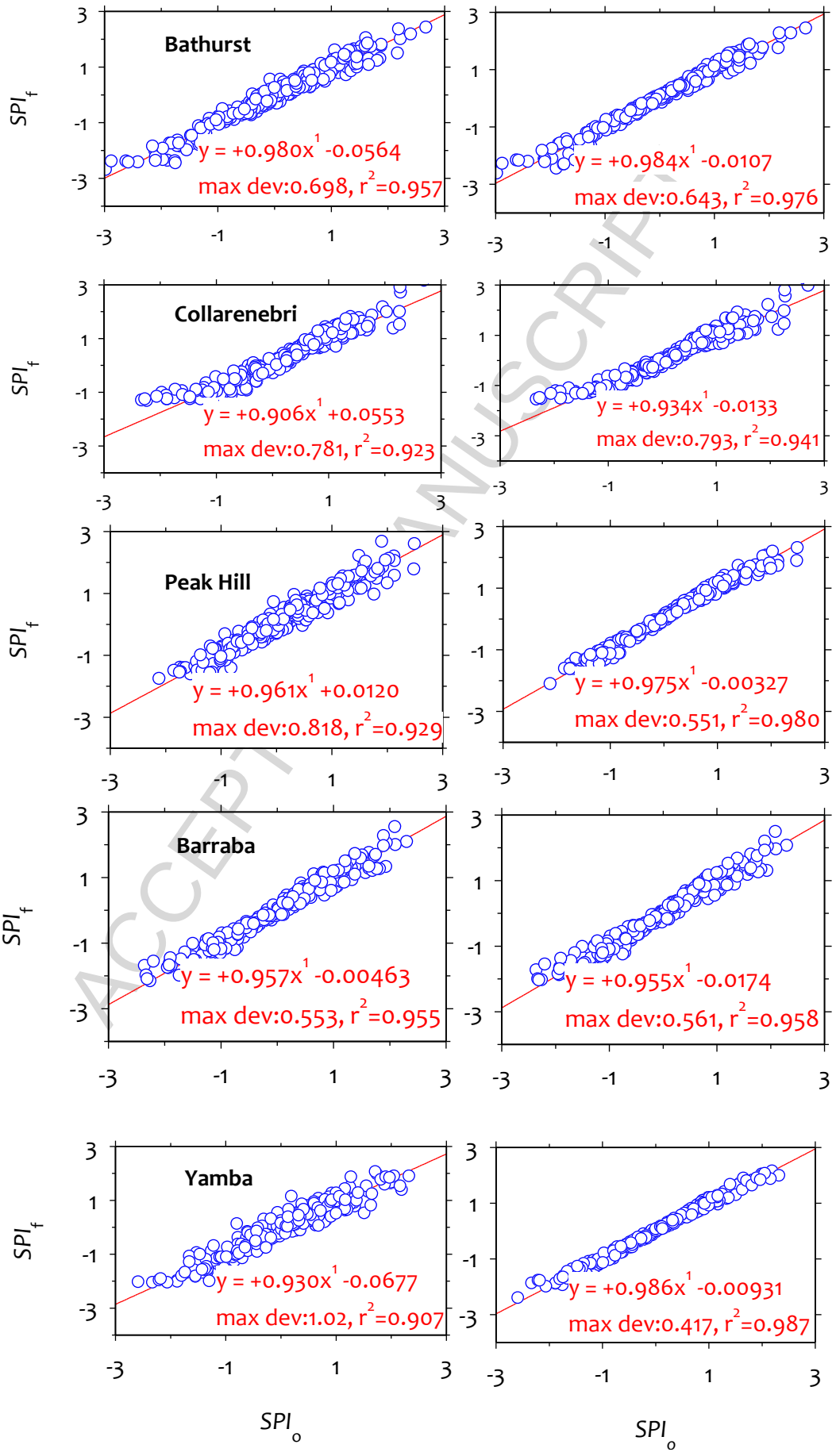

Fig. 5 Scatterplot of forecasted (SPI_F) and observed (SPI_O) standardized precipitation index (SPI) using the MARS model with and without periodicity (i.e. month) as an input parameter with a linear regression equation.

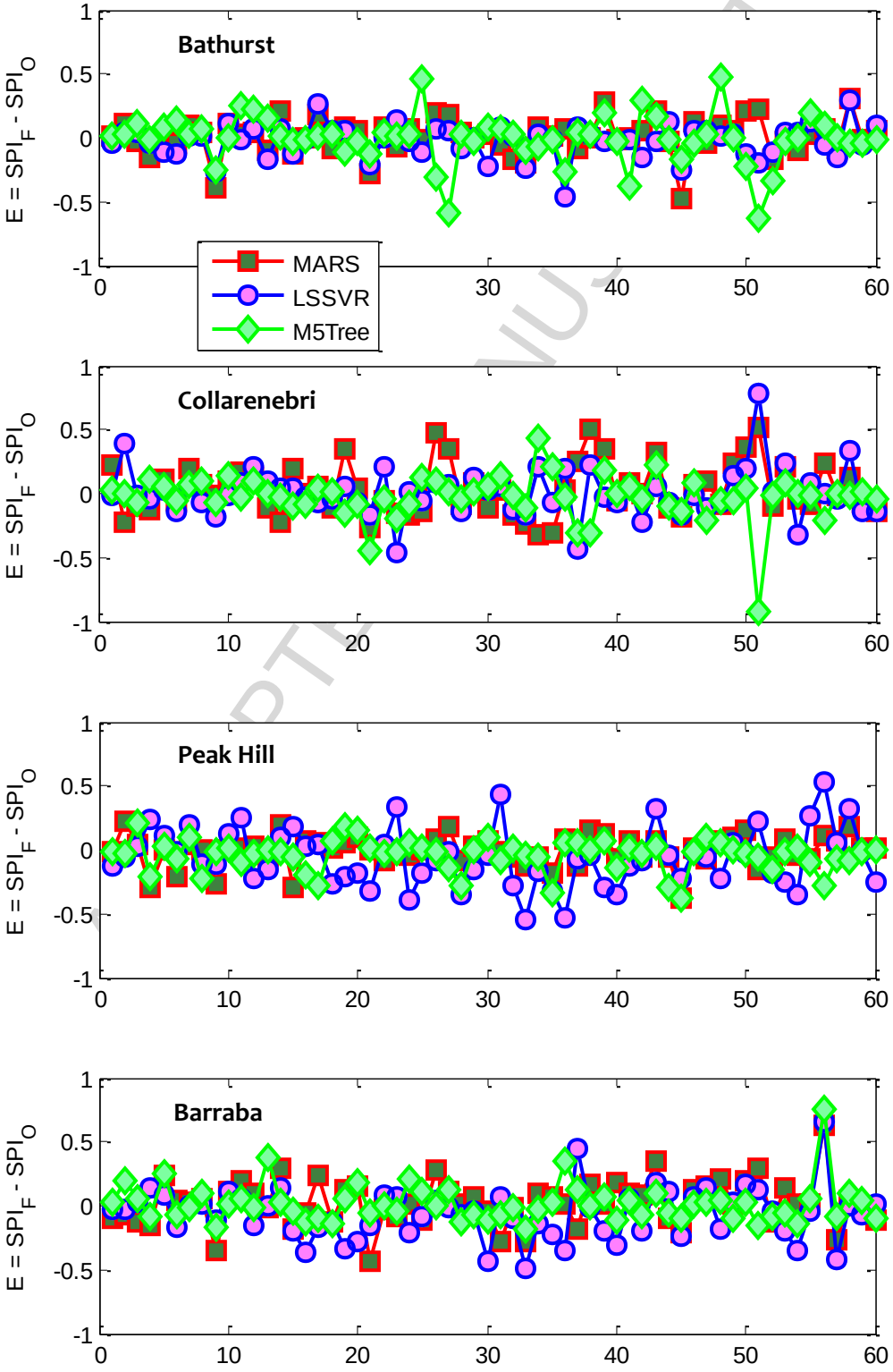

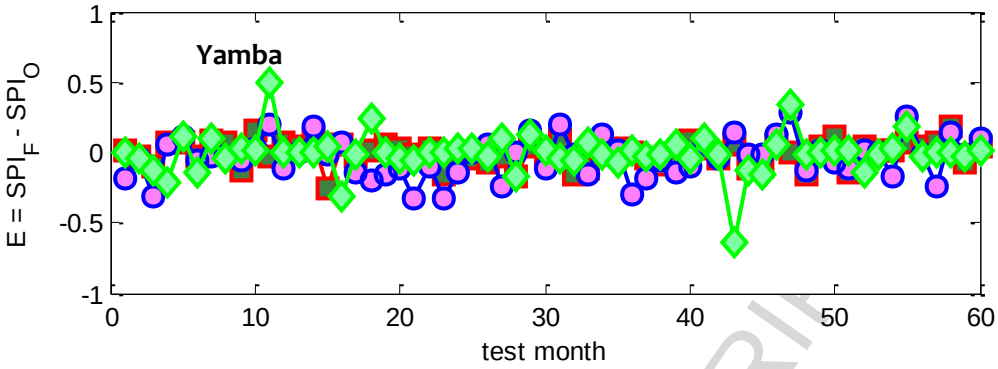

Fig. 6 Forecasting error, $E = SPI_F - SPI_O$ for MARS, LSSVM and M5Tree (with periodicity as an input variable) in the last 5 years of testing period.

Bathurst Agricultural Station

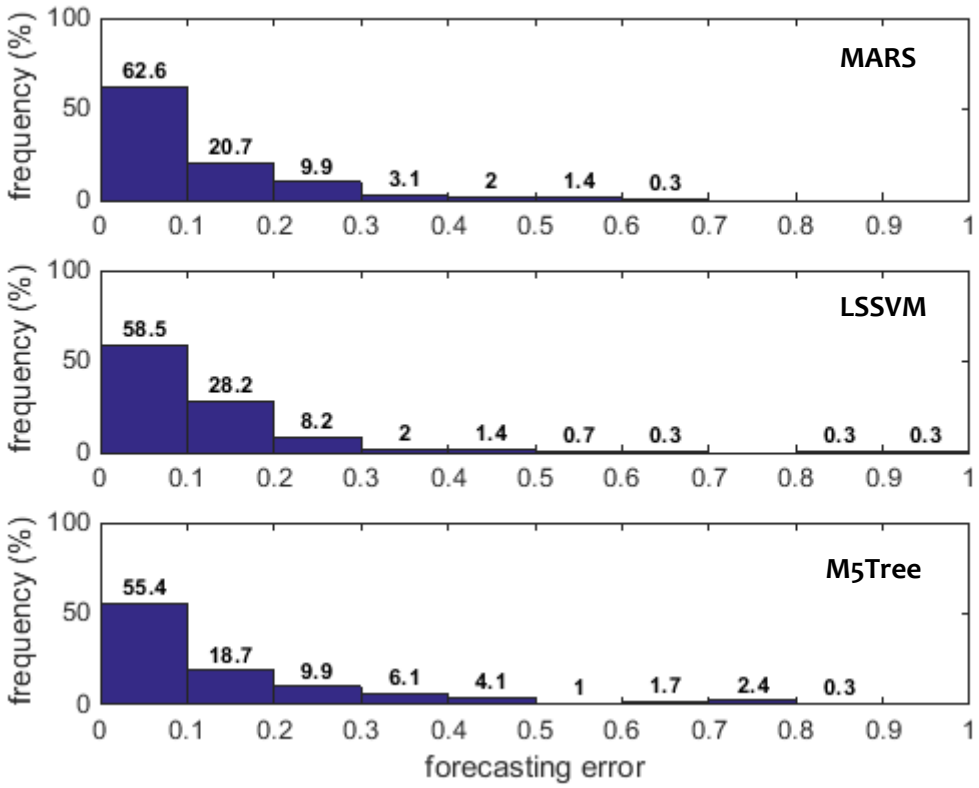

Collarenebri

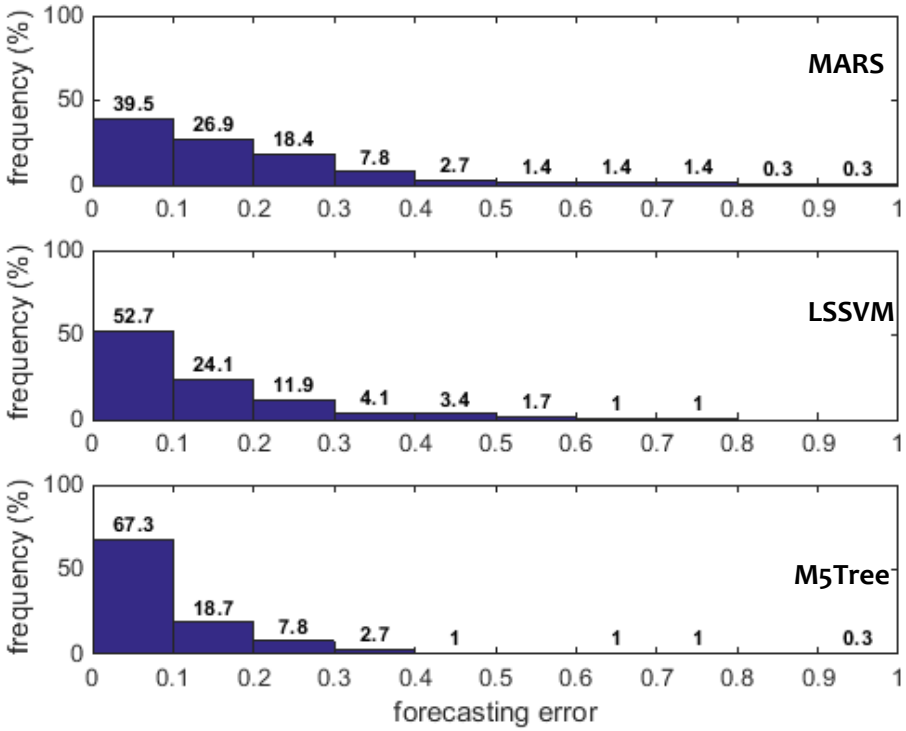

Peak Hill

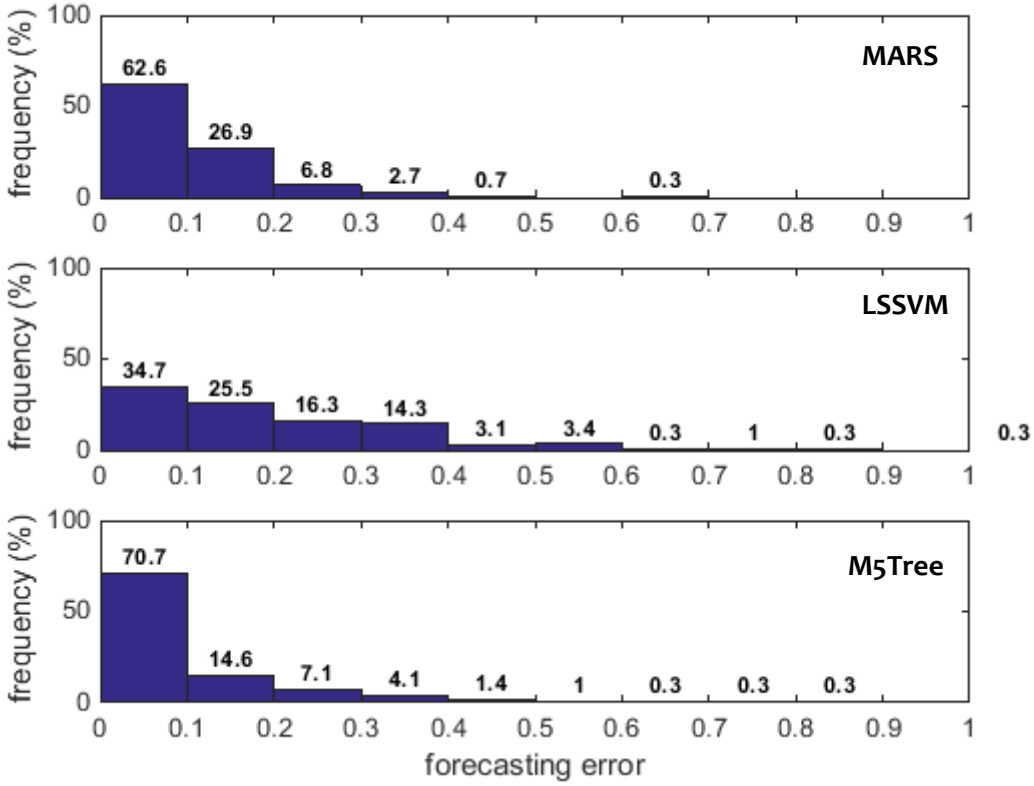

Barraba

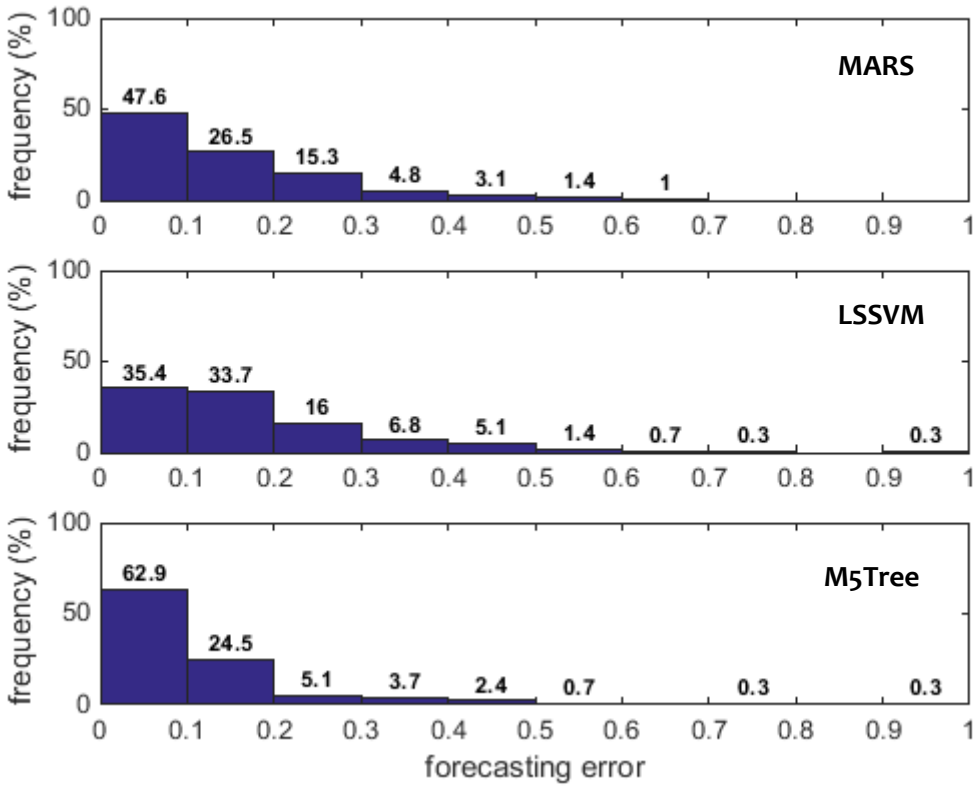

Yamba

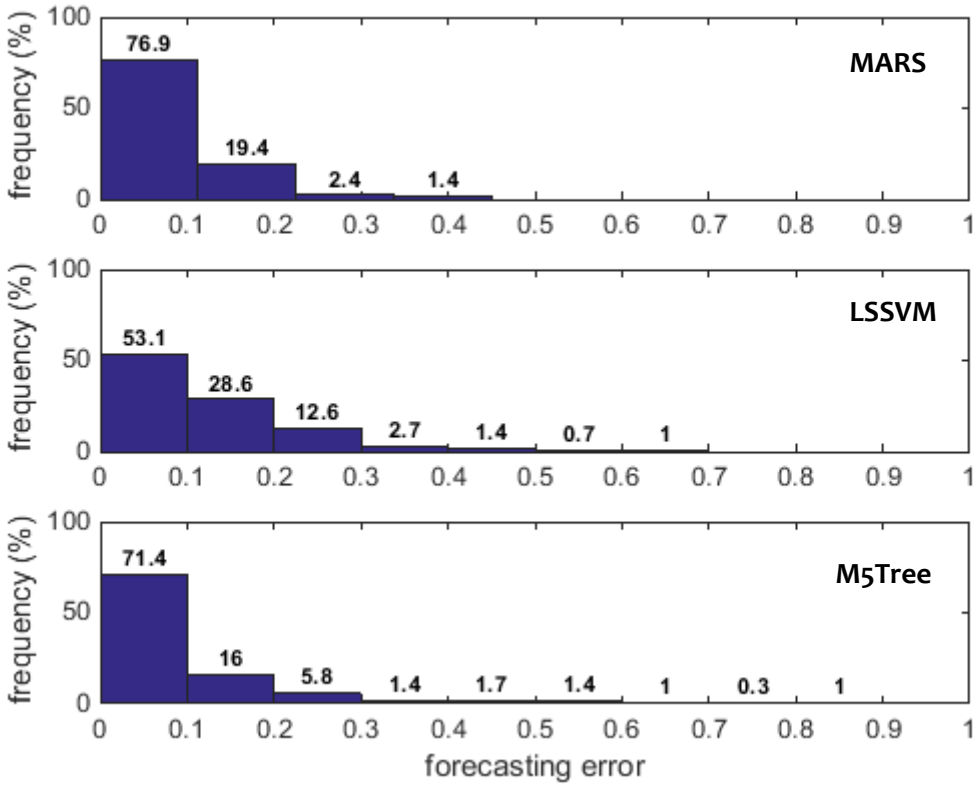

Fig. 7 Frequency distribution of forecasting error encountered by optimum MARS, LSSVM and M5Tree models.

Tables

Table 1: Descriptive statistics of the study sites.

Name of Station	Geographic Characteristics				Hydrological Statis Rainfall (*P*) r			
	ID	Long.	Lat.	Elevation (m)	Mean	Standard Deviation	Minimum	M
Bathurst Agricultural Station	63005	149.56°E	33.43°S	713	645.57	36.39	9.39	
Collarenebri (Viewpoint)	48031	148.59°E	29.55°S	145	279.77	23.93	1.06	
Peak Hill Post Office	50031	148.19°E	32.73°S	285	517.90	43.57	2.42	
Barraba Post Office	54003	150.61°E	30.38°S	500	572.74	37.15	5.36	
Yamba	58012	153.36°E	29.43°S	29	750.35	50.83	6.22	

Table 2: Input variables used for monthly *SPI* forecasting.

Variable	Acronym
Monthly Rainfall	*P*
Sea Surface Temperature	Nino3 SST
Sea Surface Temperature	Nino3.4 SST
Sea Surface Temperature	Nino4 SST
Southern Oscillation Index	SOI
Pacific Decadal Oscillation Index	PDO
Indian Ocean Dipole Index	IOD

ENSO Modoki Index	EMI

Table 3: The partitioning of input data into training, validation and testing sets.

	Number of Data Points	**Period**	**% of Data**
Total	1176	1915-2012	100
Training	588	01/1915 to 12/1963	50
Validation	294	01/1964 to 06/1988	25
Testing	294	07/1988 to 12/2012	25

Table 4: Cross correlation of inputs (with *SPI*). r_{cross} in boldface are statistically significant with 95% confidence.

Station	*P*	Nino3SST	Nino3.4SST	Nino4.0SST	SOI
Bathurst Agricultural Station	**0.897**	-0.060	**-0.094**	**-0.142**	**0.238**
Collarenebri	**0.882**	-0.041	**-0.093**	**-0.131**	**0.247**
Peak Hill	**0.833**	-0.046	**-0.093**	**-0.139**	**0.222**
Barraba	**0.884**	-0.046	**-0.112**	**-0.159**	**0.236**
Yamba	**0.854**	-0.051	**-0.088**	**-0.142**	**0.211**

Table 5: Influence of input combinations for forecasting of *SPI* using a MARS model measured by root mean square error (RMSE), mean absolute error (MAE) and coefficient of determination (R^2). Note: optimum model for each site is **boldfaced** (blue).

(a) Bathurst Agricultural Station

Input Combination	Training			Validation			Testin	
	RMSE	MAE	R^2	RMSE	MAE	R^2	RMSE	MAE
Rain	0.259	0.223	0.935	0.277	0.238	0.937	0.272	0.237
Rain,Nino3SST	0.220	0.177	0.953	0.269	0.212	0.941	0.239	0.196
Rain,Nino3SST,Nino3.4SST	0.216	0.172	0.955	0.259	0.200	0.945	0.232	0.185
Rain,Nino3SST,Nino3.4SST,Nino4SST	0.210	0.163	0.957	0.255	0.189	0.947	0.237	0.181
Rain,Nino3SST,Nino3.4SST, Nino4SST,SOI	0.205	0.161	0.959	0.243	0.184	0.952	0.222	0.174
Rain,Nino3SST,Nino3.4SST, Nino4SST,SOI,PDO	0.206	0.161	0.959	0.243	0.184	0.952	0.222	0.174
Rain,Nino3SST,Nino3.4SST, Nino4SST,SOI,PDO,IOD	0.203	0.159	0.960	0.244	0.185	0.951	0.224	0.174
Rain,Nino3SST,Nino3.4SST, Nino4SST,SOI,PDO,IOD,EMI	0.203	0.159	0.960	0.244	0.185	0.951	0.224	0.174
Rain,Nino3SST,Nino3.4SST, Nino4SST,SOI + month	**0.152**	**0.102**	**0.978**	**0.198**	**0.129**	**0.968**	**0.159**	**0.159**

(b) Collarenebri

Rain	0.276	0.216	0.907	0.287	0.212	0.904	0.286	0.20
Rain,Nino3SST	0.265	0.209	0.915	0.282	0.215	0.907	0.281	0.20
Rain,Nino3SST,Nino3.4SST	0.235	0.181	0.933	0.267	0.208	0.917	0.270	0.20
Rain,Nino3SST,Nino3.4SST,Nino4SST	0.236	0.180	0.932	0.257	0.197	0.923	0.271	0.20
Rain,Nino3SST,Nino3.4SST, Nino4SST,SOI	0.233	0.180	0.934	0.262	0.203	0.920	0.272	0.20
Rain,Nino3SST,Nino3.4SST, Nino4SST,SOI,PDO	0.233	0.180	0.934	0.262	0.203	0.920	0.272	0.20
Rain,Nino3SST,Nino3.4SST, Nino4SST,SOI,PDO,IOD	0.231	0.177	0.935	0.261	0.200	0.920	0.274	0.20
Rain,Nino3SST,Nino3.4SST, Nino4SST,SOI,PDO,IOD,EMI	0.221	0.168	0.941	0.263	0.202	0.920	0.257	0.19
Rain,Nino3SST,Nino3.4SST, Nino4SST + month	**0.205**	**0.150**	**0.949**	**0.232**	**0.167**	**0.938**	**0.234**	**0.17**

(c) Peak Hill

ain	0.297	0.252	0.903	0.310	0.256	0.895	0.298	0.
ain,Nino3SST	0.289	0.240	0.908	0.310	0.254	0.895	0.299	0.
ain,Nino3SST,Nino3.4SST	0.271	0.228	0.919	0.302	0.243	0.902	0.281	0.
ain,Nino3SST,Nino3.4SST,Nino4SST	0.260	0.215	0.926	0.284	0.224	0.912	0.270	0.
ain,Nino3SST,Nino3.4SST, Nino4SST,SOI	0.257	0.211	0.928	0.282	0.223	0.914	0.265	0.
ain,Nino3SST,Nino3.4SST, Nino4SST,SOI,PDO	0.257	0.211	0.927	0.278	0.222	0.916	0.263	0.

ain,Nino3SST,Nino3.4SST, Nino4SST,SOI,PDO,IOD	0.255	0.208	0.928	0.280	0.224	0.916	0.268	0.2
ain,Nino3SST,Nino3.4SST, Nino4SST,SOI,PDO,IOD,EMI	0.246	0.200	0.934	0.281	0.220	0.916	0.251	0.1
ain,Nino3SST,Nino3.4SST,Nino4SST, SOI, PDO, IOD, EMI + month	**0.130**	**0.096**	**0.981**	**0.148**	**0.107**	**0.976**	**0.132**	**0.0**

(d) Barraba

ain	0.213	0.162	0.955	0.244	0.163	0.946	0.218	0.1
ain,Nino3SST	0.203	0.153	0.959	0.249	0.166	0.944	0.213	0.1
ain,Nino3SST,Nino3.4SST	0.197	0.147	0.962	0.238	0.157	0.949	0.212	0.1
ain,Nino3SST,Nino3.4SST,Nino4SST	0.196	0.145	0.962	0.242	0.156	0.947	0.217	0.1
ain,Nino3SST,Nino3.4SST, Nino4SST,SOI	0.195	0.145	0.962	0.238	0.156	0.949	0.209	0.1
ain,Nino3SST,Nino3.4SST, Nino4SST,SOI,PDO	0.195	0.145	0.962	0.238	0.156	0.949	0.209	0.1
ain,Nino3SST,Nino3.4SST, Nino4SST,SOI,PDO,IOD	0.193	0.143	0.963	0.238	0.155	0.949	0.208	0.1
ain,Nino3SST,Nino3.4SST, Nino4SST,SOI,PDO,IOD,EMI	0.193	0.143	0.963	0.238	0.155	0.949	0.208	0.1
ain,Nino3SST,Nino3.4SST,Nino4SST, SOI, PDO, IOD + month	**0.188**	**0.136**	**0.965**	**0.233**	**0.145**	**0.951**	**0.202**	**0.1**

(e) Yamba

M1	Rain	0.374	0.331	0.862	0.369	0.329
M2	Rain,Nino3SST	0.351	0.300	0.878	0.360	0.304
M3	Rain,Nino3SST,Nino3.4SST	0.322	0.271	0.898	0.356	0.294
M4	Rain,Nino3SST,Nino3.4SST,Nino4SST	0.312	0.253	0.904	0.320	0.256
M5	Rain,Nino3SST,Nino3.4SST, Nino4SST,SOI	0.308	0.251	0.907	0.314	0.253
M6	Rain,Nino3SST,Nino3.4SST, Nino4SST,SOI,PDO	0.306	0.250	0.908	0.317	0.258
M7	Rain,Nino3SST,Nino3.4SST, Nino4SST,SOI,PDO,IOD	0.304	0.245	0.909	0.318	0.261
M8	Rain,Nino3SST,Nino3.4SST, Nino4SST,SOI,PDO,IOD,EMI	0.294	0.240	0.915	0.333	0.265
M9	**Rain,Nino3SST,Nino3.4SST,Nino4SST, SOI + month**	**0.108**	**0.083**	**0.988**	**0.110**	**0.081**

Table 6: Comparison of MARS, M5 Tree and LSSVM models with optimum inputs with and without periodicity.

(a) Bathurst Agricultural Station

Model	Input	Training			Validation			Test	
		RMSE	MAE	R^2	RMSE	MAE	R^2	RMSE	MAE
MARS	Rain,Nino3SST,Nino3.4SST, Nino4SST,SOI	0.205	0.161	0.959	0.243	0.184	0.952	0.222	0.174

	M5Tree	Rain,Nino3SST,Nino3.4SST, Nino4SST,SOI	0.152	0.107	0.978	0.315	0.234	0.919	0.315	0.234
	LSSVM	Rain,Nino3SST,Nino3.4SST, Nino4SST,SOI	0.205	0.158	0.959	0.257	0.186	0.947	0.223	0.171
	MARS	**Rain,Nino3SST,Nino3.4SST, Nino4SST,SOI,month**	**0.152**	**0.102**	**0.978**	**0.198**	**0.129**	**0.968**	**0.159**	**0.159**
	M5Tree	Rain,Nino3SST,Nino3.4SST, Nino4SST,SOI,month	0.109	0.062	0.989	0.244	0.150	0.951	0.244	0.150
	LSSVM	Rain,Nino3SST,Nino3.4SST, Nino4SST,SOI,month	0.124	0.086	0.985	0.195	0.126	0.970	0.159	0.109

(b) Collarenebri

	MARS	Rain,Nino3SST,Nino3.4SST, Nino4SST	0.236	0.180	0.932	0.257	0.197	0.923	0.271	0.202
	M5Tree	Rain,Nino3SST,Nino3.4SST, Nino4SST	0.166	0.117	0.967	0.288	0.207	0.903	0.288	0.207
	LSSVM	Rain,Nino3SST,Nino3.4SST, Nino4SST	0.211	0.157	0.946	0.234	0.172	0.937	0.257	0.180
	MARS	Rain,Nino3SST,Nino3.4SST, Nino4SST,month	0.205	0.150	0.949	0.232	0.167	0.938	0.234	0.172
	M5Tree	**Rain,Nino3SST,Nino3.4SST, Nino4SST,month**	**0.083**	**0.054**	**0.992**	**0.174**	**0.106**	**0.966**	**0.174**	**0.106**
	LSSVM	Rain,Nino3SST,Nino3.4SST, Nino4SST,month	0.150	0.116	0.973	0.171	0.132	0.966	0.203	0.142

(c) Peak Hill

RS	Rain,Nino3SST,Nino3.4SST, Nino4SST,SOI,PDO,IOD,EMI	0.246	0.200	0.934	0.281	0.220	0.916	0.251
Tree	Rain,Nino3SST,Nino3.4SST, Nino4SST,SOI,PDO,IOD,EMI	0.156	0.111	0.973	0.371	0.286	0.850	0.371
VM	Rain,Nino3SST,Nino3.4SST, Nino4SST,SOI,PDO,IOD,EMI	0.249	0.194	0.932	0.320	0.252	0.891	0.290
RS	**Rain,Nino3SST,Nino3.4SST,Nino4SST, SOI, PDO, IOD, EMI, month**	**0.130**	**0.096**	**0.981**	**0.148**	**0.107**	**0.976**	**0.132**
Tree	Rain,Nino3SST,Nino3.4SST,Nino4SST, SOI, PDO, IOD, EMI, month	0.087	0.054	0.992	0.209	0.109	0.955	0.209
VM	Rain,Nino3SST,Nino3.4SST,Nino4SST, SOI, PDO, IOD, EMI, month	0.175	0.135	0.967	0.283	0.198	0.917	0.279

(d) Barraba

ARS	Rain,Nino3SST,Nino3.4SST, Nino4SST,SOI,PDO,IOD	0.193	0.143	0.963	0.238	0.155	0.949	0.208
Tree	Rain,Nino3SST,Nino3.4SST, Nino4SST,SOI,PDO,IOD	0.125	0.080	0.984	0.271	0.176	0.933	0.271
SVM	Rain,Nino3SST,Nino3.4SST, Nino4SST,SOI,PDO,IOD	0.194	0.136	0.962	0.286	0.187	0.927	0.245

ARS	Rain,Nino3SST,Nino3.4SST, Nino4SST,SOI,PDO,IOD,month	0.188	0.136	0.965	0.233	0.145	0.951	0.202	
Tree	**Rain,Nino3SST,Nino3.4SST, Nino4SST,SOI,PDO,IOD,month**	**0.092**	**0.060**	**0.992**	**0.179**	**0.113**	**0.971**	**0.179**	
SVM	Rain,Nino3SST,Nino3.4SST, Nino4SST,SOI,PDO,IOD,month	0.146	0.100	0.979	0.276	0.179	0.934	0.231	

(e) Yamba

	MARS	Rain,Nino3SST,Nino3.4SST, Nino4SST,SOI	0.308	0.251	0.907	0.314	0.253	0.904	0.298
	M5Tree	Rain,Nino3SST,Nino3.4SST, Nino4SST,SOI	0.208	0.149	0.957	0.458	0.361	0.808	0.458
	LSSVM	Rain,Nino3SST,Nino3.4SST, Nino4SST,SOI	0.303	0.246	0.910	0.341	0.274	0.889	0.330
	MARS	**Rain,Nino3SST,Nino3.4SST, Nino4SST,SOI,month**	**0.108**	**0.083**	**0.988**	**0.110**	**0.081**	**0.988**	**0.107**
	M5Tree	Rain,Nino3SST,Nino3.4SST, Nino4SST,SOI,month	0.095	0.057	0.991	0.194	0.120	0.963	0.194
	LSSVM	Rain,Nino3SST,Nino3.4SST, Nino4SST,SOI,month	0.112	0.080	0.988	0.177	0.122	0.970	0.165

Table 7: Comparison of optimum MARS, LSSVM and M5Tree according to Willmott's index (*WI*) and mean absolute percentage error (MAPE, %) with and without periodicity.

Model	Without periodicity		With periodicity	
	WI	MAPE (%)	*WI*	MAPE (%)
	Bathurst Agricultural Station			
MARS	0.980	64.98	**0.989**	**29.05**
LSSVM	0.978	64.86	0.988	34.164
M5 Tree	0.967	63.82	0.977	50.860
	Collarenebri			
MARS	0.953	55.987	0.969	46.772
LSSVM	0.956	54.466	0.975	39.186
M5 Tree	0.951	52.662	**0.984**	**29.098**
	Peak Hill			
MARS	0.962	90.004	**0.990**	**25.768**
LSSVM	0.948	125.159	0.951	98.728
M5 Tree	0.925	143.911	0.985	33.920
	Barraba			
MARS	0.978	48.024	0.979	43.833
LSSVM	0.969	66.187	0.973	79.309
M5 Tree	0.968	64.151	**0.987**	**37.944**
	Yamba			
MARS	0.955	98.015	**0.994**	**22.565**
LSSVM	0.944	118.632	0.985	56.446
M5 Tree	0.916	96.837	0.984	20.897

Table 8: Forecasting skill of optimum MARS, M5Tree and LSSVM in terms of mean absolute percentage error, MAPE (%) for different categories of drought events within the test period.

(a) Moderate drought ($-1.5 \leq SPI < -0.5$).

Station	Number of Events	MARS	LSSVM	M5Tree
Bathurst Agricultural Station	52	12.9	***11.5***	15.0
Collarenebri	70	17.7	16.5	***5.9***
Peak Hill	66	11.7	18.5	**10.1**
Barraba	69	17.7	19.3	***13.6***
Yamba	60	10.9	17.6	***8.0***

(**b**) Severe drought (-2.0 ≤ *SPI* < −1.5).

Bathurst Agricultural Station	13	***6.6***	7.6	19.0
Collarenebri	8	21.2	27.1	***5.2***
Peak Hill	7	10.6	30.6	***5.1***
Barraba	11	5.9	11.4	***3.0***
Yamba	16	***1.3***	10.3	2.3

(**c**) Extreme drought (-2.0 < *SPI*).

Bathurst Agricultural Station	10	11.5	19.2	***7.3***
Collarenebri	5	30.9	32.2	***11.8***
Peak Hill	1	***0.2***	37.2	4.9
Barraba	6	9.1	16.0	***8.1***
Yamba	5	12.9	19.3	***10.6***

Table 9: Analysis of mean absolute percentage error, MAPE (%), over seasonal scales.

Season	MARS	LSSVM	M5 Tree
	Bathurst Agricultural Station		
DJF	25.4	61.3	25.7
MAM	17.4	44.0	36.1
JJA	31.2	66.7	33.6
SON	39.6	28.7	34.8
	Collarenebri		
DJF	45.7	45.3	27.3
MAM	31.2	24.0	23.7
JJA	33.5	27.7	20.7
SON	79.6	62.0	45.3
	Peak Hill		
DJF	27.2	89.7	9.8
MAM	45.7	80.1	69.4
JJA	20.0	98.2	41.2
SON	11.6	131.3	17.9
	Barraba		
DJF	37.3	61.8	36.6
MAM	36.7	73.9	27.4
JJA	29.2	91.4	29.5
SON	71.3	89.1	59.1
	Yamba		
DJF	23.7	49.1	13.7
MAM	17.7	53.8	30.4

JJA	18.6	39.1	21.4
SON	30.7	86.4	19.1

Appendix

Table A1 The regression tree for the optimal MARS models in modeling SPI-Bathurst.

```
if (x6 <= 34) then f1_1 = -(x6 - (43))
if (34 < x6 < 65) then begin
  f1_1 = -0.0042*(x6-(65))^2 – 4.3637e-004*(x6-(65))^3
end
if (x6 >= (65)) then f1_1 = 0
BF1 = f1_1
if (x1 <= 3) then f2_1 = -(x1 - (4))
if (3 < x1 < 8) then begin
  f2_1 = -0.08*(x1-(8))^2 – 0.024*(x1-(8))^3
end
if (x1 >= (8)) then f2_1 = 0
BF2 = f2_1
if (x6 <= 11) then f3_1 = 0
if (11 < x6 < 20) then begin
  f3_1 = 0.037*(x6-(11))^2 + 0.0014*(x6-(11))^3
end
if (x6 >= (20)) then f3_1 = x6 - (16)
BF3 = f3_1
if (x6 <= 65) then f4_1 = -(x6 - (86))
if (65 < x6 < 1.5e+002) then begin
  f4_1 = -0.003*(x6-(1.5e+002))^2 – 7.0018e-005*(x6-
(1.5e+002))^3
end
if (x6 >= (1.5e+002)) then f4_1 = 0
```

```
BF4 = f4_1

if (x6 <= 0.9) then f5_1 = 0

if (0.9 < x6 < 3.7) then begin

  f5_1 = 0.3699*(x6-(0.9))^2 – 0.0456*(x6-(0.9))^3

end

if (x6 >= (3.7)) then f5_1 = x6 - (1.8)

BF5 = f5_1

if (x6 <= 3.7) then f6_1 = 0

if (3.7 < x6 < 11) then begin

  f6_1 = 0.167*(x6-(3.7))^2 – 0.009*(x6-(3.7))^3

end

if (x6 >= (11)) then f6_1 = x6 - (5.6)

BF6 = f6_1

if (x5 <= -25) then f7_1 = 0

if (-25 < x5 < 8.1) then begin

  f7_1 = 0.044*(x5-(-25))^2 – 5.8183e-004*(x5-(-25))^3

end

if (x5 >= (8.1)) then f7_1 = x5 - (-19)

BF7 = f7_1

if (x6 <= 20) then f8_1 = 0

if (20 < x6 < 34) then begin

  f8_1 = 0.0663*(x6-(20))^2 – 0.0015*(x6-(20))^3

end

if (x6 >= (34)) then f8_1 = x6 - (25)

BF8 = f8_1

if (x6 <= 20) then f9_1 = -(x6 - (25))

if (20 < x6 < 34) then begin
```

```
  f9_1 = 0.051*(x6-(34))^2 – 0.0015*(x6-(34))^3
end
if (x6 >= (34)) then f9_1 = 0
BF9 = f9_1
if (x1 <= 1.5) then f10_1 = 0
if (1.5 < x1 < 3) then begin
  f10_1 = 0.6667*(x1-(1.5))^2 – 0.1481*(x1-(1.5))^3
end
if (x1 >= (3)) then f10_1 = x1 - (2)
BF10 = f10_1
if (x4 <= 27) then f11_1 = -(x4 - (28))
if (27 < x4 < 29) then begin
  f11_1 = 0.25*(x4-(29))^2
end
if (x4 >= (29)) then f11_1 = 0
BF11 = f11_1

y = -8.4 - 0.012*BF1 - 0.28*BF2 - 0.011*BF3 -
0.013*BF4 + 0.52*BF5 - 0.15*BF6 + 0.0029*BF7 -
0.35*BF8 + 0.34*BF9 - 0.084*BF10 - 0.13*BF11
```

Table A2. The regression tree for the optimal M5Tree models in modeling SPI-Bathurst.

```
if x6 <= 42.7
 if x6 <= 19.85
  if x6 <= 10.15
   if x6 <= 4.45
    if x5 <= -6.45
```

```
    y = -2.75428571428571 (7)
   else
    if x5 <= 1.45
     y = -2 (7)
    else
     y = -2.55156171284635 + 0.0459613769941225*x1 (8)
  else
   y = 7.6005572677018 + 0.0311186393304645*x1 + 0.249128501454831*x2 - 0.583489121310296*x4
+ 0.0772307128297949*x6 (26)
 else
  if x1 <= 6.5
   if x6 <= 12.45
    y = -1.305 (4)
   else
    if x1 <= 2.5
     y = -1.082 (5)
    else
     if x4 <= 28.8
      if x6 <= 16.3
       y = -0.83 (6)
      else
       y = -0.734285714285714 (7)
     else
      y = -0.9525 (8)
  else
   if x6 <= 15.95
    if x6 <= 14.2
```

```
    y = -1.58555555555556 (9)
   else
    y = -1.384 (5)
  else
   if x1 <= 8.5
    y = -1.11 (6)
   else
    y = -2.01509601181684 +0.0432078643100904*x6 (14)
else
 if x6 <= 29.7
  if x1 <= 7.5
   if x6 <= 23
    y = -4.9906418424715 +0.16339975807993*x2 (13)
   else
    if x2 <= 26.91
     if x2 <= 25.475
      y = -0.595 (4)
     else
      y = 2.94136136490269 -0.128186361112679*x2 (12)
    else
     y = -1.0250676828162 +0.025908183632735*x6 (11)
  else
   if x6 <= 22.95
    y = -1.0625 (8)
   else
    if x4 <= 28.485
     y = -0.832 (5)
```

```
  else
   y = -0.732727272727273 (11)
else
 if x2 <= 26.155
  if x6 <= 39
   if x1 <= 9.5
    if x1 <= 3.5
     y = -0.574285714285714 (7)
    else
     if x6 <= 34.9
      if x3 <= 26.555
       y = -0.48 (4)
      else
       if x4 <= 28.49
        y = -0.298 (5)
       else
        y = -0.426 (5)
     else
      if x6 <= 35.8
       y = -0.278333333333333 (6)
      else
       y = -0.136 (5)
   else
    y = -1.69505221221408 +0.0328222875807718*x6 (19)
  else
   if x1 <= 9.5
    y = -0.113333333333333 (12)
```

```
    else
     y = -0.361666666666667 (6)
   else
    if x6 <= 35.25
     if x4 <= 28.415
      y = -0.125555555555556 (9)
     else
      y = -0.224 (10)
    else
     if x1 <= 2.5
      y = -0.134 (5)
     else
      if x5 <= 2.75
       y = -0.0951622219572619 -0.027771153769723*x5 (9)
      else
       y = 0.195 (4)
else
 if x6 <= 71.15
  if x6 <= 59.2
   if x2 <= 26.29
    if x1 <= 9.5
     if x1 <= 1.5
      if x3 <= 26.32
       y = 0.0175 (4)
      else
       y = -0.125 (4)
     else
```

```
    y = -1.09477396421314 +0.0207946091353223*x1 +0.0232968613926662*x6 (31)
   else
    y = -1.41947811310633 -0.00265541177638728*x5 +0.0265583293265269*x6 (17)
  else
   if x6 <= 46.65
    y = 0.279851166123848 +0.015308016065288*x5 (11)
   else
    if x1 <= 3.5
     y = 0.295 (6)
    else
     y = -0.935799976862525 +0.0276984035168896*x6 (14)
 else
  if x1 <= 9.5
   if x1 <= 2.5
    y = 0.32875 (8)
   else
    if x6 <= 66.85
     if x1 <= 3.5
      y = 0.53 (5)
     else
      if x2 <= 25.775
       if x4 <= 28.04
        y = 0.68 (4)
       else
        y = 0.554 (10)
      else
       y = 0.74375 (8)
```

```
    else
     if x3 <= 26.71
      y = 0.8875 (4)
     else
      y = -3.522795793917 +0.155716895525512*x3 (9)
   else
    if x1 <= 11.5
     y = -0.926616718430315 +0.0189454936190883*x6 (11)
    else
     y = -1.19196682216042 +0.0211240106923831*x6 (9)
else
 if x6 <= 105.25
  if x1 <= 3.5
   y = -0.913263577756861 +0.15450568679058*x1 +0.0155988481396871*x6 (27)
  else
   if x1 <= 9.5
    if x6 <= 82.8
     if x6 <= 79.95
      if x2 <= 26.54
       y = 5.03526987602692 -0.144862251159137*x4 (10)
      else
       y = 1.04666666666667 (9)
     else
      y = 1.13 (6)
    else
     if x6 <= 92.15
      if x1 <= 7.5
```

```
      y = 1.287 (10)
     else
      y = 1.2025 (4)
    else
     y = 1.50214285714286 (14)
  else
   y = 0.386808224487173 -0.115578532673103*x1 +0.0182463170369555*x6 (29)
else
 if x6 <= 153.75
  if x5 <= 5.4
   if x1 <= 3
    y = 1.0175 (4)
   else
    y = 1.37428571428571 (7)
  else
   if x4 <= 28.36
    y = 1.48133333333333 (15)
   else
    y = 1.915 (4)
 else
  if x4 <= 28.535
   y = 1.9375 (8)
  else
   y = 2.3425 (4)
```

Research Highlights

1. Standardized Precipitation Index was modelled using MARS, LSSVM and M5Tree with rainfall, climate indices and SST as predictor variables.
2. MARS and M5Tree models outperformed LSSVR, and highlighted the importance of periodicity as a predictor variable for SPI-modelling.
3. Drought forecasting was dependent on proper combination of predictor variables and scaled with the geographic location of study sites.